A High-Resolution Stable Isotope Analysis of Middle Eocene Planktonic Foraminifera

Christopher Bowman

Senior Thesis in Geology & Geophysics

Adviser: Dr. Pincelli Hull

29 April 2016

Abstract

The calcium carbonate test geochemistry of planktonic foraminifera is an important paleoceanographic tool, but little is known about the ability of these organisms to record short-term, orbital-scale environmental change, especially during the ice-free Eocene. This study compiles high-resolution stable isotope ($\delta^{13}C$ and $\delta^{18}O$) records for two species of planktonic foraminifera (*Acarinina bullbrooki* and *Subbotina eocaena*) across a 400 kyr window of long-term climate stability during the Middle Eocene (~42 Ma). The planktonic carbon and oxygen isotope records produced in this study show a high degree of stability across the interval, with a faint obliquity signal in the carbon records and no significant orbital cyclicity in the oxygen records. These results suggest that $\delta^{13}C$ DIC may have been significantly more variable than surface ocean temperature during the Eocene. The magnitude of $\delta^{18}O$ variability suggests that planktonic foraminiferal populations do not engage in habitat tracking over millennial timescales. Discrepancy between benthic and planktonic foraminiferal stable isotope patterns suggests that either benthic or planktonic foraminifera may not reliably track orbital-scale surface ocean chemistry and temperature change. These results raise important uncertainties and call for further investigation into the paleoecology of planktonic foraminifera over millennial timescales.

1. Introduction

In recent decades, planktonic foraminifera have gained increasing significance as a paleoceangraphic tool (Emiliani, 1954; Spero, 1998; Ezard *et al.*, 2015). The carbon and oxygen isotopes preserved in their calcium carbonate tests are utilized as indicators of temperature, productivity and carbonate chemistry of past oceans (Pearson *et al.*, 1993; Pearson *et al.*, 2012; Birch *et al.*, 2013). Planktonic foraminifera can provide information about surface and thermocline waters, supplementing well-established deep water analyses conducted using benthic foraminifera. The extraction of meaningful environmental information from fossilized planktonic foraminiferal tests is not, however, without its challenges. Recent work has indicated that the test chemistry of these organisms does not only trace environmental conditions, but is also influenced by biological, ecological and postmortem processes (Killingley *et al.*, 1980; Spero & Williams, 1988; Birch *et al.*, 2013; Ezard *et al.*, 2015).

The utility of planktonic foraminifera as a paleooceanographic tool rests largely in their ability to record seawater geochemistry in specific depth habitats through the water column (Birch *et al.*, 2013; John *et al.*, 2013). Specifically, $\delta^{18}O$ is used to infer ocean temperature and the depth habitats of planktonic foraminifera, given that the oxygen composition of seawater generally shifts towards heavier ^{18}O as temperature decreases and depth increases (Pearson *et al.*, 2012). Carbon isotopes can provide valuable information about productivity and nutrient recycling in surface or near surface waters (John *et al.*, 2013). The photosynthetic production of organic matter preferentially removes lighter ^{12}C from the surface DIC reservoir, thus increasing $\delta^{13}C$ in shallower waters with high primary productivity (John *et al.,* 2013; Marsay *et al.*, 2015). Foraminiferal calcite records the carbon isotopes of seawater DIC, thus recording high $\delta^{13}C$ values in surface waters and low $\delta^{13}C$ values in deep waters where organic matter rich in ^{12}C is decomposed (John *et al.*, 2013). The recycling of lighter ^{12}C as organic carbon sinks through the thermocline enables information about nutrient recycling rates to be extracted from comparisons of planktonic foraminifera living at different depth habitats (Marsay *et al.*, 2015). The efficiency of this "biological pump," or the transport of organic carbon from the surface ocean to the deep ocean before it is remineralized back into CO_2, can significantly impact atmospheric CO_2 concentrations (John *et al.*, 2013; Marsay *et al.*, 2015).

The environment-isotope relationships in planktonic foraminifera described above, however, are complicated by an array of biological and ecological factors. These factors,

historically referred to by the blanket term "vital effects," include ontogenic, metabolic and seasonal effects, as well as the potential effects of photosymbiosis (Erez & Honjo, 1981; Killingley *et al.*, 1981; Spero *et al.*, 1992; Spero *et al.*, 1997; Wade *et al.*, 2008). Recent efforts have primarily focused on intraspecific body size-isotope trends within narrow time windows (e.g. Elderfield *et al.*, 2002; Bornemann & Norris, 2007, Birch *et al.*, 2013; Ezard *et al.*, 2015). This work has greatly increased our understanding of physiological effects on planktonic foraminiferal test chemistry, but much less is known about how population dynamics influence the geochemical signal recorded on longer timescales.

Not typically included on lists of biological "vital effects" is the potential ability of planktonic foraminiferal communities to adjust to or buffer short term environmental changes. The extent to which such communities can track ecological niches in response to orbital-forced climate variation (via movement through the water column, for instance) remains largely unexplored. Past studies have demonstrated high intra-annual variability (around 2‰) in both $\delta^{13}C$ and $\delta^{18}O$ between individual specimens of planktonic foraminifera of the same species (Killingley *et al.*, 1981; Reynolds & Thunell, 1985; Sautter & Thunell, 1991; Spero & Williams, 1989). This variability, largely hypothesized to be seasonality-driven, is of much greater magnitude than the variability found between individual specimens within benthic foraminiferal populations (Fallet *et al*., 2010; Wit *et al*., 2010). This discrepancy suggests that planktonic foraminifera may have greater potential as recorders of short-term environmental change, but further research at the population level is required to either support or refute this claim. An absence of high resolution stable isotope data for planktonic foraminifera has contributed to the lack of investigation in this area. Recent sample collection efforts by the International Ocean Discovery Program (IODP), however, have produced high resolution Cenozoic sediment records, opening new avenues for exploring planktonic foraminiferal ecology (Norris *et al.*, 2014).

In particular, the recent IODP Expedition 342 (Paleogene Newfoundland Sediment Drifts) has produced a high resolution Northern Atlantic sedimentary record through the Paleogene (Norris *et al.*, 2014). Within this interval, the Eocene Epoch (~55.5 – 35 Ma) is of particular interest for high resolution climate studies, as past Eocene studies have exclusively focused on describing long term climate trends or anomalies using data of coarse resolution (e.g. Zachos *et al.*, 2001; Pearson *et al.*, 2007; Burgess *et al.*, 2008; D'Haenens *et al.*, 2012). The relative climatic effects of various orbital cycles during the warm, ice-free Eocene remains

largely unknown (Zachos *et al.*, 2001; Hull *et al.*, 2013). While benthic foraminiferal $\delta^{18}O$ records indicate that obliquity-driven (~40 kyr) orbital cycles had the most significant impact on short term climate during the later Cenozoic, Zachos *et al.* (2001) expressed uncertainty about the relative dominance of obliquity-forced climatic variation during the ice-free Eocene. The newly collected high-resolution planktonic foraminiferal records from this time period, in addition to their potential for ecological analysis, also present an unprecedented opportunity for studying orbital-forced climate change during the Eocene.

This study aims to evaluate the sensitivity of planktonic foraminiferal communities to orbital climate cycles across a short (approximately 400 kyr) interval in the middle Eocene using stable carbon and oxygen isotopes. The results of stable isotope analyses also provide insight into the effects of short-term climate cyclicity on ocean temperature and carbon and nutrient remineralization patterns. The chosen interval encompasses a time of relative long-term temperature stability with high-magnitude orbital effects on broad scale environmental conditions (indicated by proxies such as x-ray fluorescence Ca/Al and Si/Ti measurements). Furthermore, the mid- to high-latitude location of the sample site used in this study may enable the detection of stronger orbital-based cycles in productivity and biological pump function (Rohling *et al.*, 2012). The isotopic analysis conducted in this study enables observation of the sensitivity of planktonic foraminifera to such orbital cycles in relation to patterns of broader environmental change.

2. Objectives

The overall goal of this study is to use stable carbon and oxygen isotope data to evaluate the sensitivity of planktonic foraminifera to background, orbital-driven climate fluctuations during a period of long-term climate stability in the middle Eocene. In order to assess $\delta^{13}C$ and $\delta^{18}O$ water column gradients, two species of different depth habitats were chosen (*Acarinina bullbrooki*, a symbiont-bearing surface mixed layer dweller, and *Subbotina eocaena*, a thermocline dweller, from Pearson *et al.*, 2006). Stable isotope results indicate the extent to which these representative surface and thermocline species record environmental variation in $\delta^{18}O$ and $\delta^{13}C$ over orbital timescales. Isotope results from *A. bullbrooki* provide information about sea surface temperatures, and comparison with measurements from the deeper *S. eocaena* will provide information about temperature gradients and biological pump efficiency (Hilting *et*

al., 2008). The isotope data obtained in this study is evaluated in the context of other sediment indices such as x-ray fluorescence (XRF) metal ratios (productivity proxies) and the relative abundance of foraminifera within the sediments (coarse fraction).

This study is designed to investigate several broad regions of uncertainty related to orbital-forced climate change and planktonic foraminiferal ecology. First, we aim to determine the extent to which planktonic foraminifera can accommodate short-term climate change via biological mechanisms or by adjusting depth habitat. While past studies of fossil planktonic foraminifera have produced much larger intra-sample ranges in both $\delta^{18}O$ and $\delta^{13}C$ than have been found in benthic foraminifera (Killingley *et al.*, 1981; Spero, 1992), studies of seasonal variation in living planktonic foraminifera have produced far different results. Seasonal variability in $\delta^{13}C$ for live planktonic foraminifera tends to be highly damped or nonexistent, suggesting that these communities may be adjusting to short term environmental change (Williams *et al.*, 1980; Sautter & Thunell, 1991; Tedesco *et al.*, 2007; Mohtadi *et al.*, 2009; Fallet *et al.*, 2010; Wit *et al.*, 2010; Hull *et al.*, 2011). This study aims to investigate the ability of planktonic foraminiferal communities to similarly adapt to climate change on longer orbital timescales.

Given the high intraspecific isotope variability described above, this study also aims to determine the extent to which orbital-scale climate change can be extracted from background isotope variability in planktonic foraminifera. Past studies have suggested that a large number of individual specimens are required to extract precise and reliable stable isotope data from planktonic foraminiferal populations (Schiffelbein & Hills, 1984; Ganssen *et al.*, 2011). The use of two distinct sampling methodologies in this study facilitates direct observation of the effects of sample size on planktonic foraminiferal stable isotope analysis. Roughly one third of the stable isotope measurements in this study are taken from samples of three to five whole specimens, while the remaining measurements are made on aliquots from samples of around thirty specimens. In addition to determining the reliability and potential utility of planktonic foraminifera as environmental indicators over millennial timescales, this study also enables a direct comparison of two sampling techniques widely used in planktonic foraminiferal research.

Finally, our results enable a direct comparison of the variability of surface and thermocline waters versus deep waters on orbital timescales during the warm Eocene. Given the high-latitude location of our sample site, it is expected that surface waters should show higher

orbital-forced temperature variability and more high-frequency variability than deep waters (data for which will be obtained from benthic foraminiferal records). Results from this study are also compared to similar middle Eocene datasets from both low- and high-latitude sites to produce a more complete picture of short-term ocean temperature variability during the Eocene.

3. Materials & Methods

3. 1 Sample Selection and Preparation

Samples were analyzed from the Integrated Ocean Drilling Program (IODP) site U1408, which is a mid-depth site from the Expedition 342 Paleogene Newfoundland sediment drifts depth transect (Norris *et al.*, 2014). One sieve size fraction was analyzed for 104 samples from an approximately 11 m thick interval of site U1408 (119.52-130.84 meters composite depth (mcd), corresponding to an age of approximately 42 Ma). Linear sedimentation rates in this interval are approximately 3 cm/kyr, so the inferred resolution for this dataset is 3-4 kyr. The first 44 samples (119.52-123.84 mcd) were taken from hole U1408B (lat. 41°26.2989′N; long. 49°47.1361′W; 3022.1 m present water depth); the next 29 samples (123.92-127.28 mcd) were taken from hole U1408C (lat. 41°26.2878′N; long. 49°47.1345′W; 3022.5 m present water depth); the final 31 samples (127.36-130.84 mcd) were taken from hole U1408A (lat. 41°26.2985′N; long. 49°47.1483′W; 3033.2 m present water depth). All three holes are contained in the same lithostratigraphic unit and show similar physical and biogenic properties, composed primarily of greenish gray nannofossil clays of Oligocene to middle Eocene age.

Carbon and oxygen stable isotope measurements were made on monospecific samples of well-preserved *Acarinina bullbrooki* and *Subbotina eocaena* Scanning electron microscope images of each species were taken by Simon D'haenens and Paige Breen to analyze preservation. The narrow size window of 250-300 μm was chosen to minimize potential artifacts from size dependent "vital effects," which are shown to be at a minimum in the 212-355 μm size window for symbiotic surface-dwelling and thermocline-dwelling foraminifera (D'Hondt *et al.*, 1994; Elderfield *et al.*, 2002; Friedrich *et al.*, 2012; Birch *et al.*, 2013). Prior to isotope analysis, each sample was washed 2 to 3 times. The first wash consisted of soaking the sample in deionized water for 24 hours, followed by rinsing and sieving on a >63 μm sieve with deionized water. Sodium metaphosphate solution, a boron-free, pH-buffered clay disaggregant, was used in the second wash cycle.

In addition, 28 samples (dispersed throughout the entire study interval) were cleaned for trace metal analysis prior to stable isotope measurements. This procedure consisted of rinsing and cleaning the samples via ultrasonication three times in Milli-Q water. The samples were then soaked in an oxidative mixture in a hot water bath for five minutes, followed by ultrasonication, and this process was also repeated three times. The samples were then rinsed an additional three times with Milli-Q water. Aliquots of between 45 and 75 μg were taken from the cleaned samples for stable isotope analysis.

3.2 Stable Isotope Analysis

Stable isotope measurements were made on the first 37 samples (119.52-123.00 mcd) in Spring 2015. For these samples, between 3 and 5 whole specimens were used for each measurement to obtain a sample mass of between 45 and 75 μg. All specimens were cleaned ultrasonically for 1 to 3 seconds prior to isotopic analysis. Duplicate isotopic measurements were taken for all samples, and triplicate measurements were taken for 12 samples to evaluate analytical precision and potential within-sample variation. Stable isotope measurements were made using a Kiel IV Carbonate Device with a Thermo MAT 253 dual-inlet mass spectrometer housed at Yale University. Precision was better than 0.017‰ for $\delta^{13}C$ and better than 0.032‰ for $\delta^{18}O$, based on two standards: NBS19 and in-house reference TS, corrected to V-PDB.

The remaining 67 samples (123.12-130.84 mcd), along with 9 overlapping repeat samples (122.1-123.00 mcd), were measured in Spring 2016. For all of these samples, an average of 30 specimens were cleaned ultrasonically and then crushed between glass microscope slides. Aliquots of between 45 and 75 μg were taken from the crushed samples and used for stable isotope measurements.

Stable isotope measurements were made on 44 of the 76 aliquot samples using a Kiel IV Carbonate Device with a Thermo MAT 253 dual-inlet mass spectrometer housed at Yale University. Analytical precision was high, with values similar to those presented above for the samples measured in 2015. Stable isotope measurements were made on the remaining 32 aliquot samples, along with 11 repeat samples for offset correction, using a Kiel IV Carbonate Device with a Thermo MAT 253 isotope ratio mass spectrometer housed at the University of California, Santa Cruz Stable Isotope Laboratory. Analytical precision was high, with similar values to those produced by measurements conducted at Yale. A complete sample list with sampling method,

preparation, and measurement location information can be found in Table 5 in the Appendix.

Planktonic stable isotope measurements are compared with coarse fraction weight percent data from Hull *et al.* (2015). Bulk sediment and benthic stable isotope records, as well as XRF Ca/Al data, were obtained by Simon D'haenens (unpublished).

4. Results

4.1 Preservation

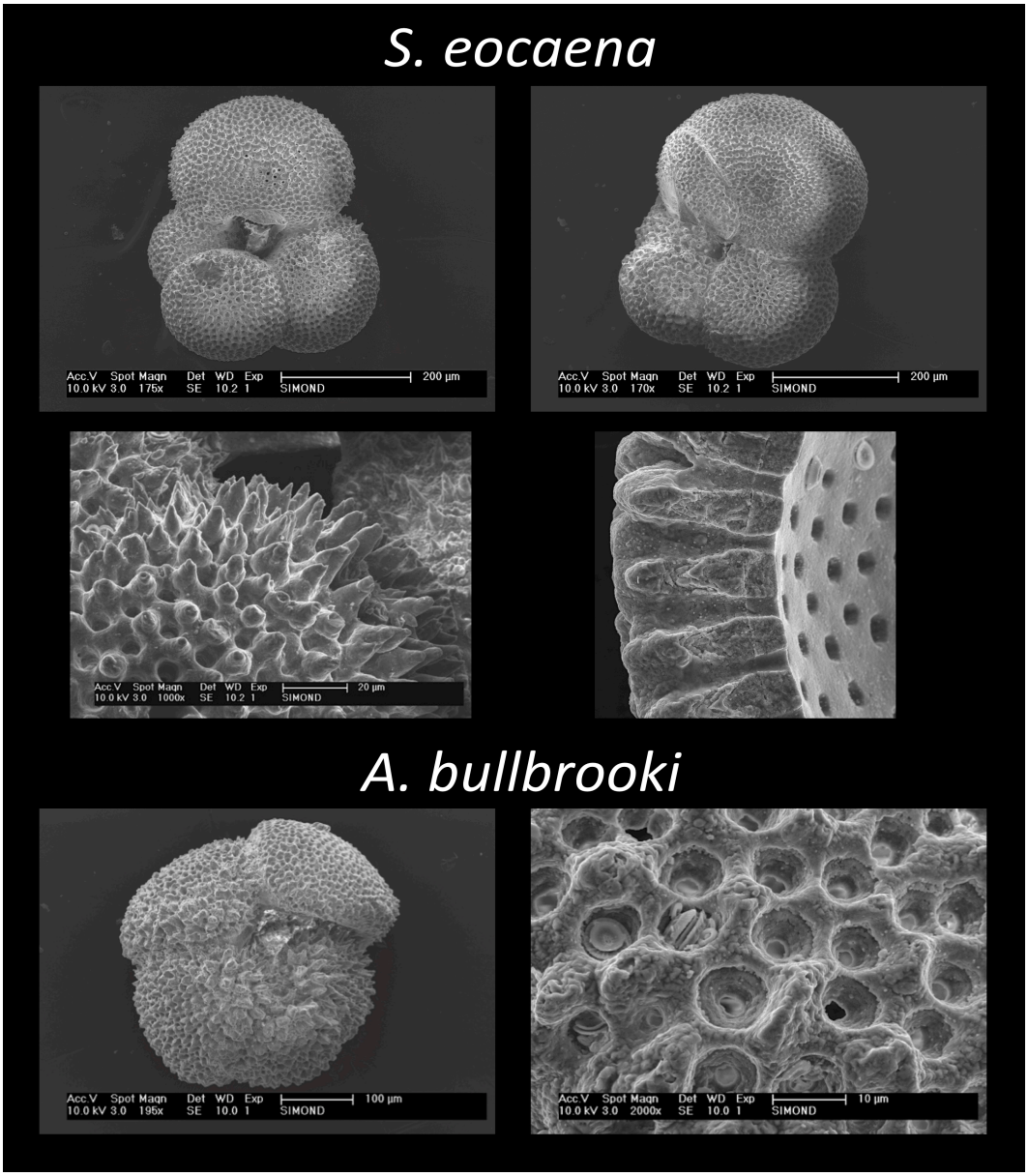

Figure 1. SEM images of *Subbotina eocaena* and *Acarinina bullbrooki*. TOP ROW: *S. eocaena* specimen with average preservation for study interval; MIDDLE ROW: calcite overgrowth on *S. eocaena* test wall (*left*), cross section of well-preserved *S. eocaena* test wall (*right*); BOTTOM ROW: *A. bullbrooki* specimen (*left*), *A. bullbrooki* test wall with some diagenetic calcite (*right*).Images were acquired by Simon D'haenens and Paige Breen.

Figure 1 displays scanning electron microscope (SEM) images of *S. eocaena* and *A. bullbrooki* specimens from the shallower portion of the study interval (approximately mcd 120). These specimens are representative of the typical preservation conditions found throughout the study interval, which could be characterized as good to very good, with minimal diagenetic alteration. The middle row depicts the range of preservation quality found for *S. eocaena*, from moderate calcite overgrowths in the left image to almost no diagenetic alteration in the right image. Preservation for *S. eocaena* remained good throughout the study interval, with no noticeable changes in test wall texture and only minor fluctuations in species abundance in the samples. The bottom row of Figure 1 depicts typical preservation conditions for *A. bullbrooki*, with some diagenetic calcite evident in both images. Preservation of *A. bullbrooki* was generally good throughout the interval, with noticeably poor preservation only encountered in a short sequence of six samples, from 125.96 to 126.56 mcd. The relative abundance of *A. bullbrooki* within the 250-300 μm size fraction was significantly reduced for these six samples, resulting in smaller sample sizes for stable isotope analysis. As shown in Figure 2, this limitation does not appear to have produced unusual stable isotope results for these six samples.

4.2 Stable Isotope Results

Figure 2 shows the results of stable isotope measurements ($\delta^{13}C$ and $\delta^{18}O$) for *A. bullbrooki* and *S. eocaena* across the entire study interval. These results are plotted alongside benthic foraminiferal and bulk sediment stable isotope, XRF Ca/Al and weight percent coarse fraction records. A preliminary visual analysis of Figure 2 suggests that the planktonic foraminiferal stable isotope records did not mirror the strong cyclicity seen in the coarse fraction and XRF data. The shaded bars on Figure 2 are aligned with peaks in coarse fraction weight percent. These peaks appear to align at certain points with patterns in the benthic and bulk sediment stable isotope records (especially in the bulk $\delta^{13}C$ record, for example). The shaded bars do not, however, appear to align with any clear peak and trough patterns seen in the planktonic datasets. The overall variability of the planktonic records does not exceed an approximate magnitude of 1‰ across the entire study interval. This variability is similar in magnitude to that of other Eocene planktonic foraminiferal stable isotope datasets (a more complete comparison is provided in Section 4.4).

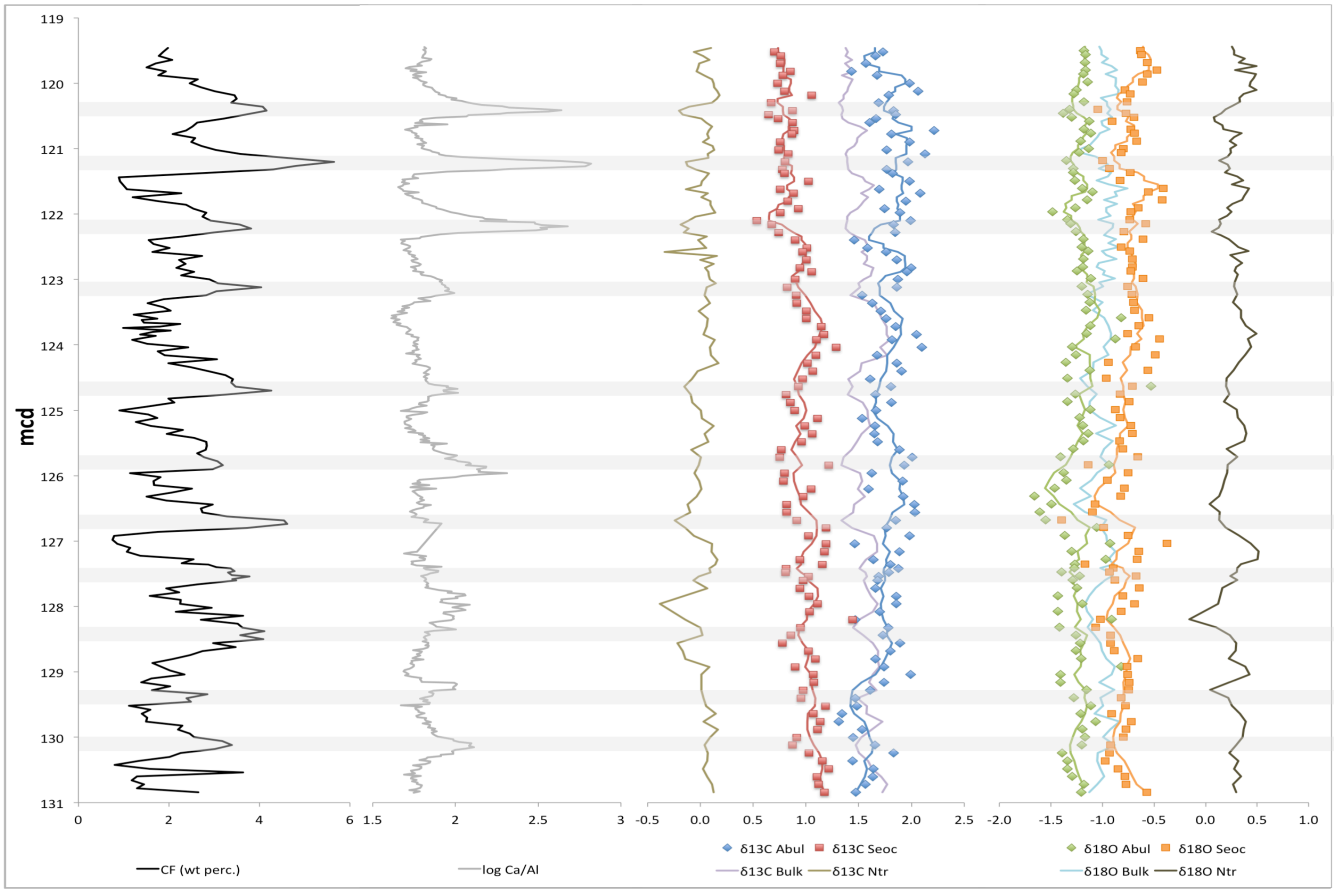

Figure 2. Stable isotope records for *A. bullbrooki* and *S. eocaena* plotted versus depth (mcd), along with coarse fraction weight percentage (from Hull *et al.* 2015), and XRF Ca/Al measurements, bulk sediment isotope records and benthic foraminifera (*N. trumpeyi*) stable isotope records (from Simon D'haenens, unpublished data). Data points represent averages wherever duplicate or triplicate samples were measured. Lines for planktonic foraminiferal datasets represent 5-sample running averages. Shaded bars represent approximate coarse fraction peaks.

The relative stability seen in the planktonic records must be put in the context of the variability observed in the other stable isotope records. The bulk $\delta^{13}C$ and $\delta^{18}O$ records both show a high degree of stability across the study interval, with total ranges of less than 0.5‰. The benthic records (*N. trumpeyi*) show total ranges under 1‰ across the interval. Table 1 provides standard deviation values for each stable isotope record. These values were calculated from the residuals of each dataset after linear de-trending to remove long-term patterns. *A. bullbrooki* shows the highest variability in both $\delta^{13}C$ and $\delta^{18}O$, followed closely by *S. eocaena*. The benthic (*N. trumpeyi*) and bulk sediment records show significantly reduced variability in comparison. The variability statistics produced here are compared to those of other planktonic and benthic foraminiferal datasets in Section 4.4.

	A. bullbrooki	*S. eocaena*	*N. trumpeyi*	Bulk Sediment
SD $\delta^{13}C$	0.172	0.133	0.107	0.099
SD $\delta^{18}O$	0.160	0.159	0.111	0.094

Table 1. Standard deviations of stable isotope records, calculated from residuals of linearly de-trended datasets.

To directly compare patterns and relationships between the isotope records produced in this study, gradients were calculated between the planktonic records and between each planktonic record and the bulk and benthic records. Figure 3 displays the $\delta^{13}C$ and $\delta^{18}O$ gradients between *A. bullbrooki* and *S. eocaena* across the study interval. No clear trend is visible in the oxygen isotopes (shown in red), but a gradual increasing trend is visible in the carbon isotope gradient, with *A. bullbrooki* $\delta^{13}C$ becoming more positive relative to *S. eocaena* $\delta^{13}C$ across the interval.

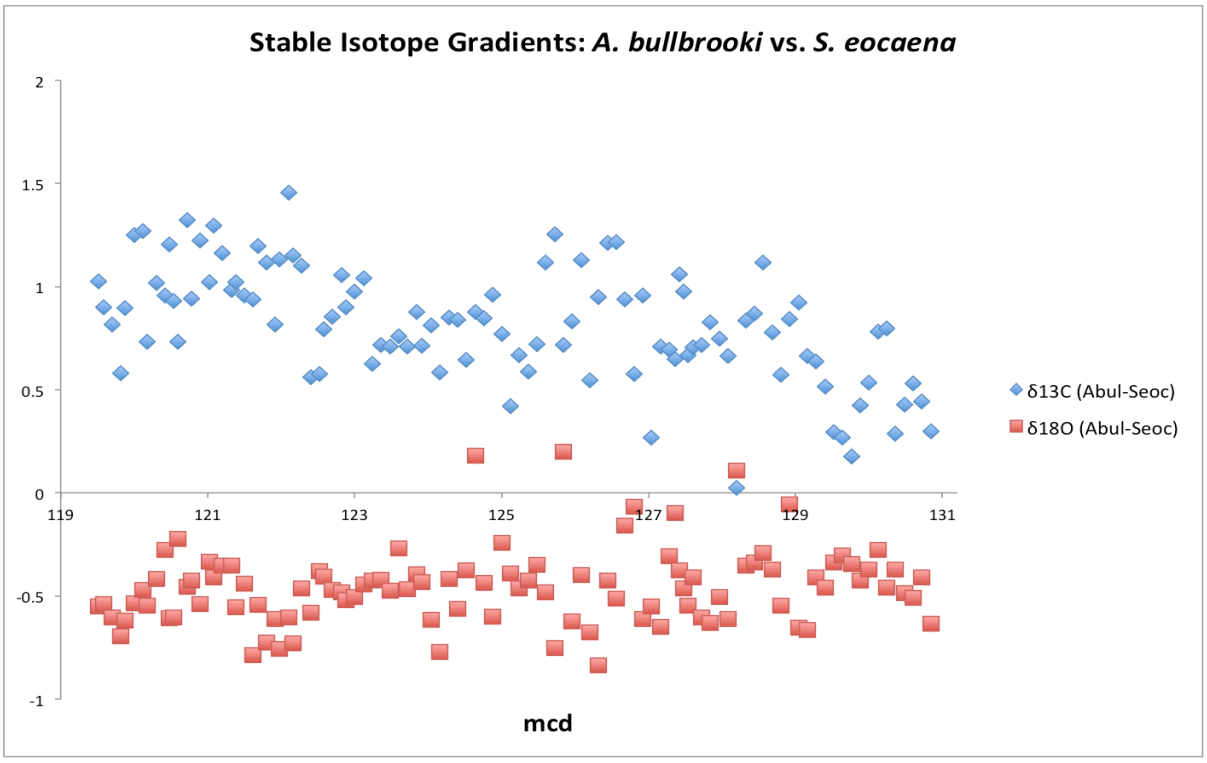

Figure 3. Stable isotope gradients ($\delta^{13}C$ in blue, $\delta^{18}O$ in red) between *A. bullbrooki* and *S. eocaena*. Gradients calculated based on average measurements wherever duplicate samples were measured.

Figures 4 and 5 show the stable isotope gradients calculated between *A. bullbrooki* and the bulk and benthic stable isotope records, respectively. The gradients displayed in Figure 4 suggest no clear trend in relative $\delta^{18}O$ values between *A. bullbrooki* and the bulk record. The carbon gradient does, however, show a gradual increasing trend across the study interval, with *A. bullbrooki* $\delta^{13}C$ becoming elevated in comparison to the bulk values at shallower depths. The

gradients produced in Figure 5 suggest a relatively constant offset between *A. bullbrooki* and *N. trumpeyi* $\delta^{13}C$ and $\delta^{18}O$ values across the study interval.

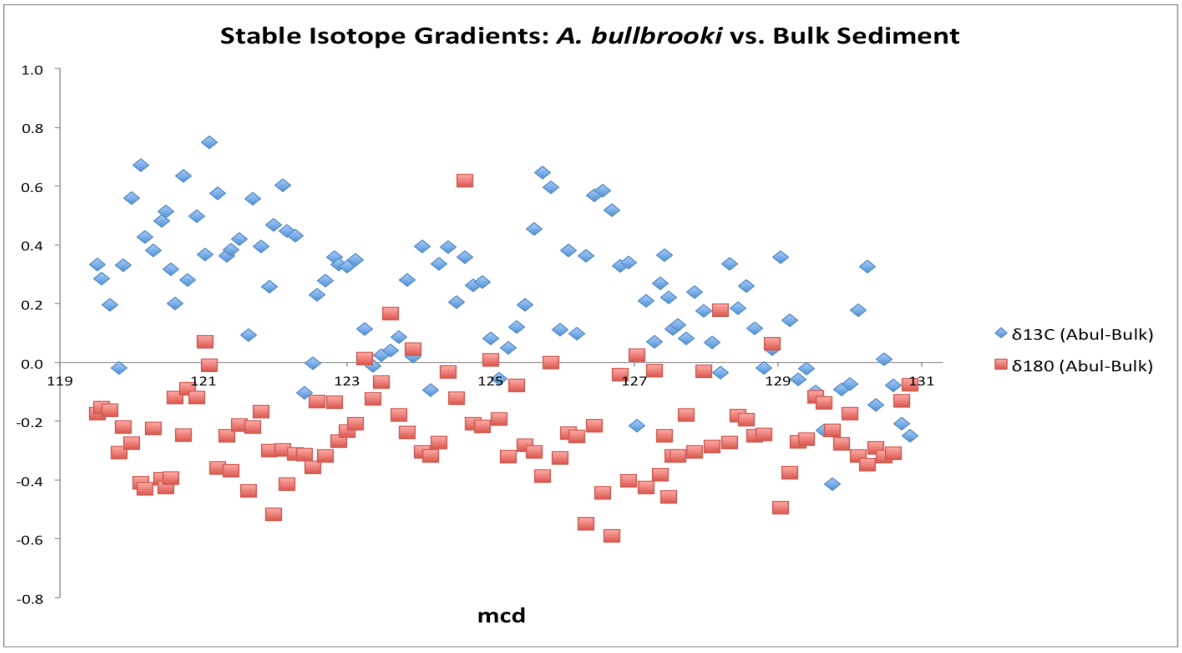

Figure 4. Stable isotope gradients ($\delta^{13}C$ in blue, $\delta^{18}O$ in red) between *A. bullbrooki* and the bulk sediment record. Gradients calculated based on average measurements wherever duplicate samples were measured.

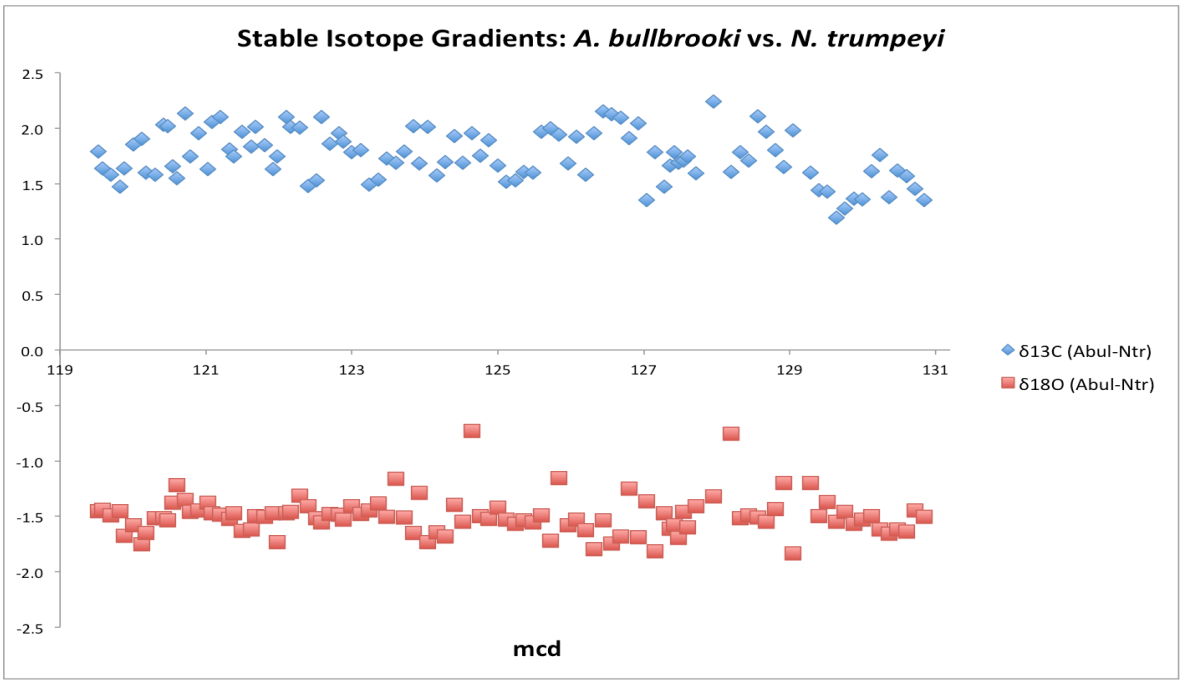

Figure 5. Stable isotope gradients ($\delta^{13}C$ in blue, $\delta^{18}O$ in red) between *A. bullbrooki* and *N. trumpeyi* (benthic). Gradients calculated based on average measurements wherever duplicate samples were measured.

Figures 6 and 7 show the stable isotope gradients calculated between *S. eocaena* and the bulk sediment and benthic stable isotope records, respectively. Both the $\delta^{13}C$ and $\delta^{18}O$ gradients

displayed in Figure 6 suggest a relatively constant offset between *S. eocaena* and bulk sediment records across the study interval, with no clear increasing or decreasing trends in either gradient. The $\delta^{13}C$ gradient depicted in Figure 7 suggests a slight declining trend in the offset between *S. eocaena* and the benthic (*N. trumpeyi*) record across the study interval, with a slight increasing trend apparent in the equivalent $\delta^{18}O$ gradient.

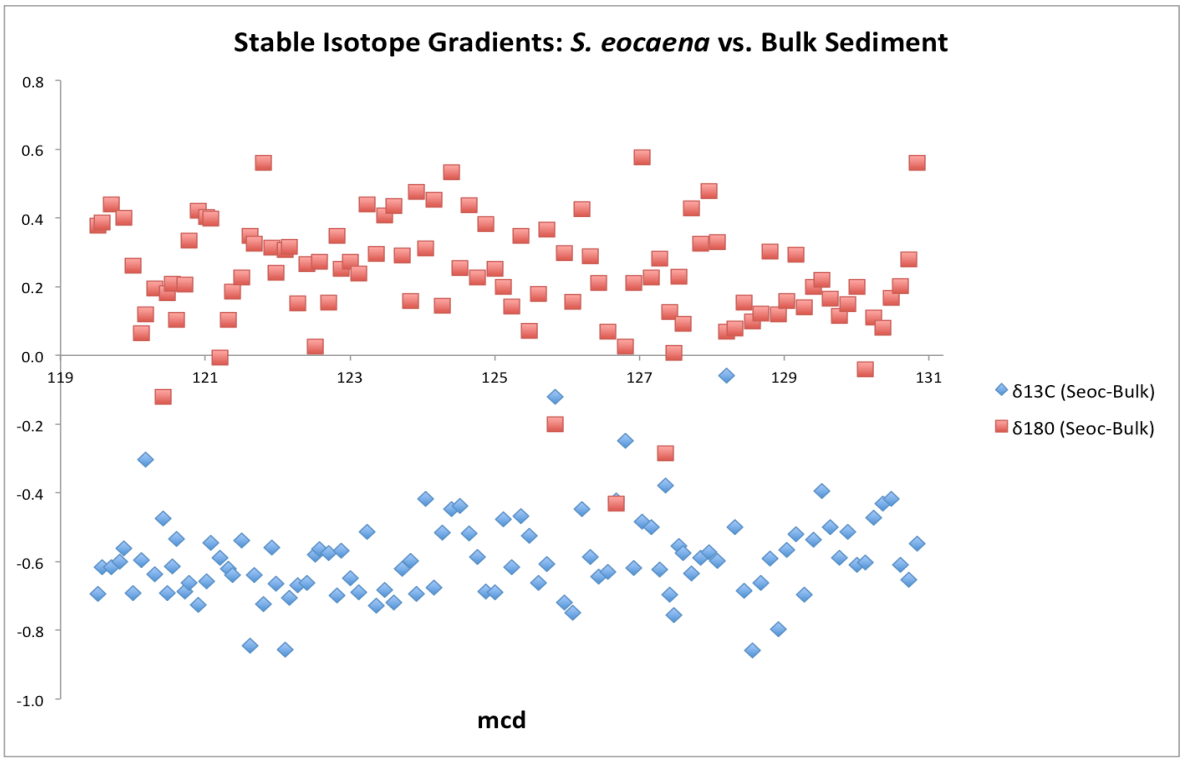

Figure 5. Stable isotope gradients ($\delta^{13}C$ in blue, $\delta^{18}O$ in red) between *S. eocaena* and the bulk sediment record. Gradients calculated based on average measurements wherever duplicate samples were measured.

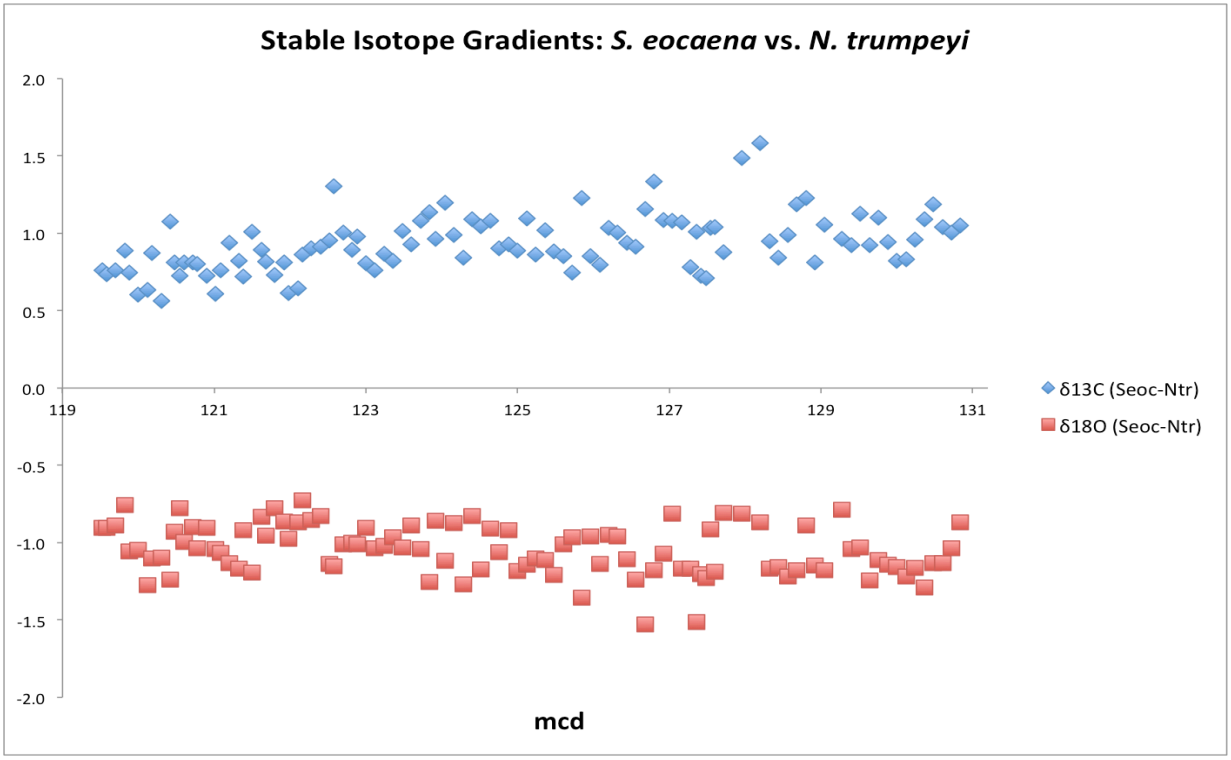

Figure 7. Stable isotope gradients ($\delta^{13}C$ in blue, $\delta^{18}O$ in red) between *S. eocaena* and *N. trumpeyi* (benthic). Gradients calculated based on average measurements wherever duplicate samples were measured

In order to fully determine the relationship between each planktonic record and the bulk sediment record, the *A. bullbrooki* and *S. eocaena* records are plotted directly against the bulk data, and a linear regression is performed to determine the relative significance of each relationship. Figures 8 and 9 show the *A. bullbrooki* $\delta^{13}C$ and $\delta^{18}O$ records, respectively, plotted against the equivalent bulk sediment records. The relationship between these two records is extremely weak, as suggested by the low R^2 values for both regression calculations (0.02 and 0.04, respectively). Figures 10 and 11 show the *S. eocaena* $\delta^{13}C$ and $\delta^{18}O$ records, respectively, plotted against the equivalent bulk sediment records. The correlation between these two records is stronger than the relationship between the *A. bullrooki* and bulk records. The *S. eocaena* and bulk $\delta^{13}C$ records were most strongly correlated, with an R^2 value of 0.38. The $\delta^{18}O$ records produced an R^2 value of 0.09, which, while higher than the equivalent calculation for *A. bullbrooki*, still suggests an extremely weak correlation. Overall, these results suggest that the bulk stable isotope records more closely track the records of the thermocline-dwelling *S. eocaena* than the surfaced-mixed-layer dwelling *A. bullbrooki*.

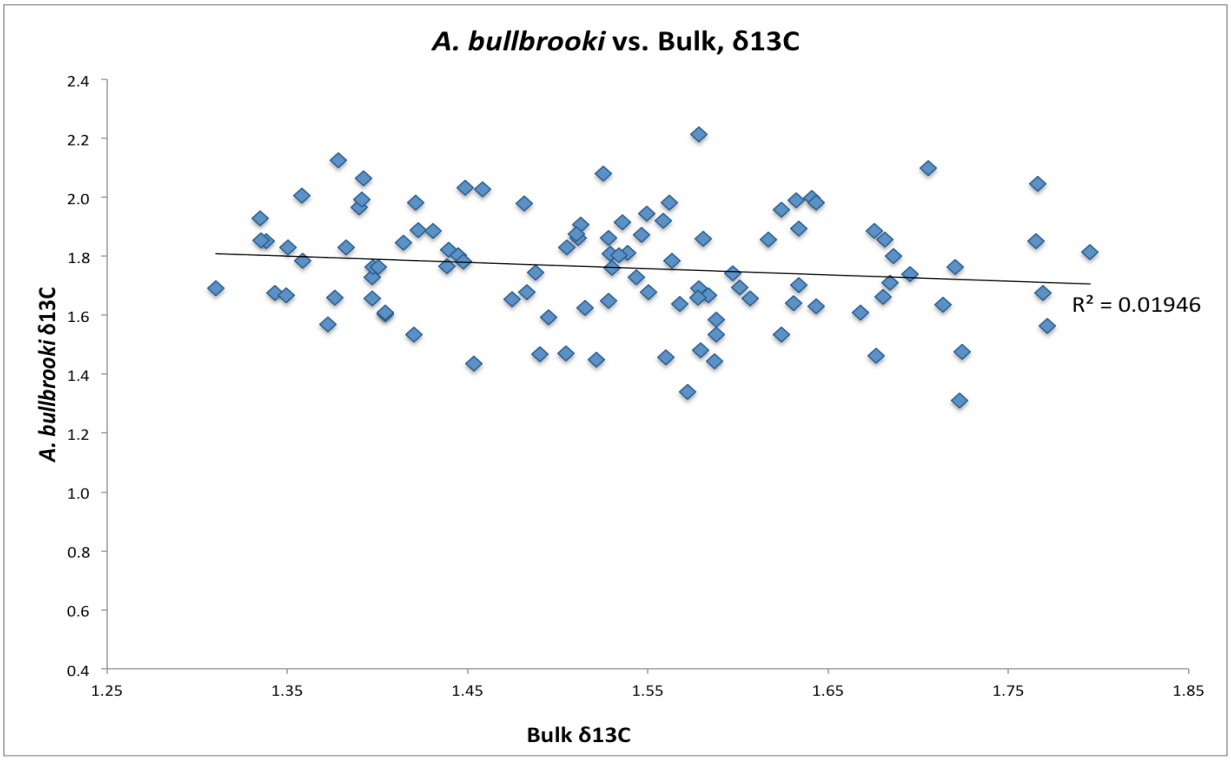

Figure 8. *A. bullbrooki* $\delta^{13}C$ results plotted against bulk sediment $\delta^{13}C$ results. A linear regression was performed on the dataset and the resulting R^2 value is provided on the chart.

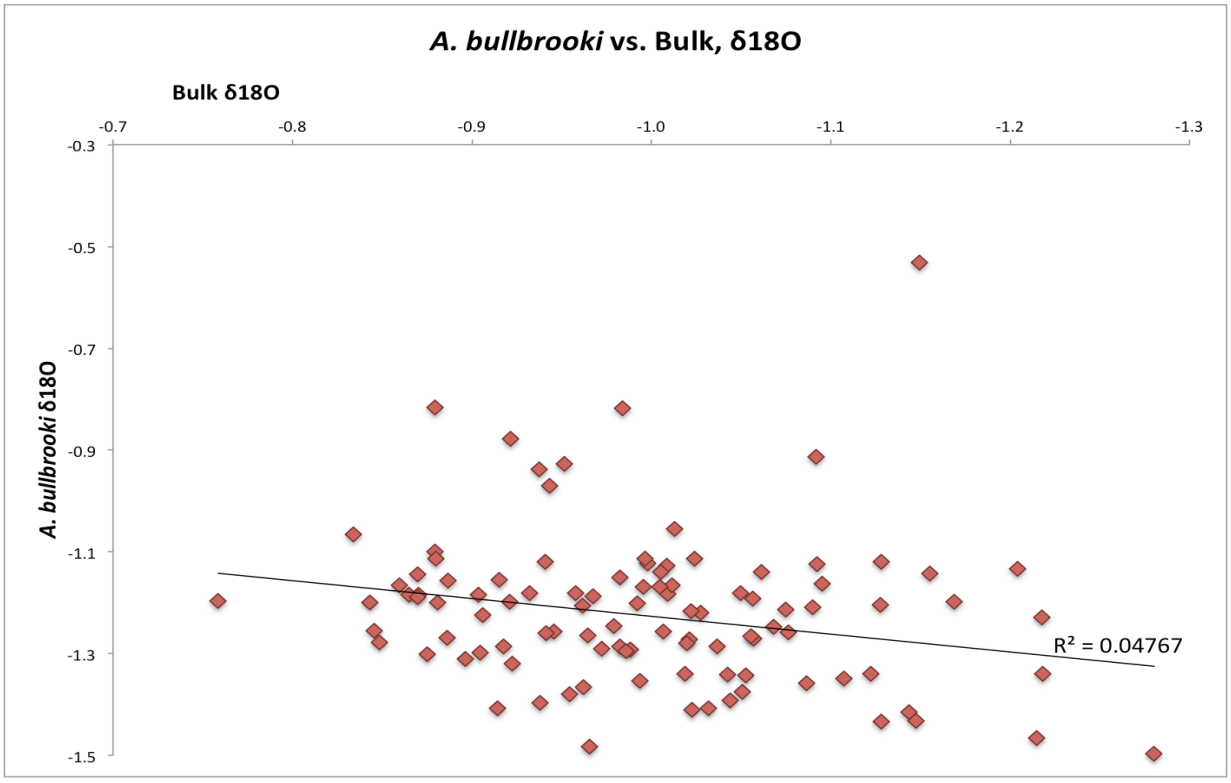

Figure 9. *A. bullbrooki* $\delta^{18}O$ results plotted against bulk sediment $\delta^{18}O$ results. A linear regression was performed on the dataset and the resulting R^2 value is provided on the chart.

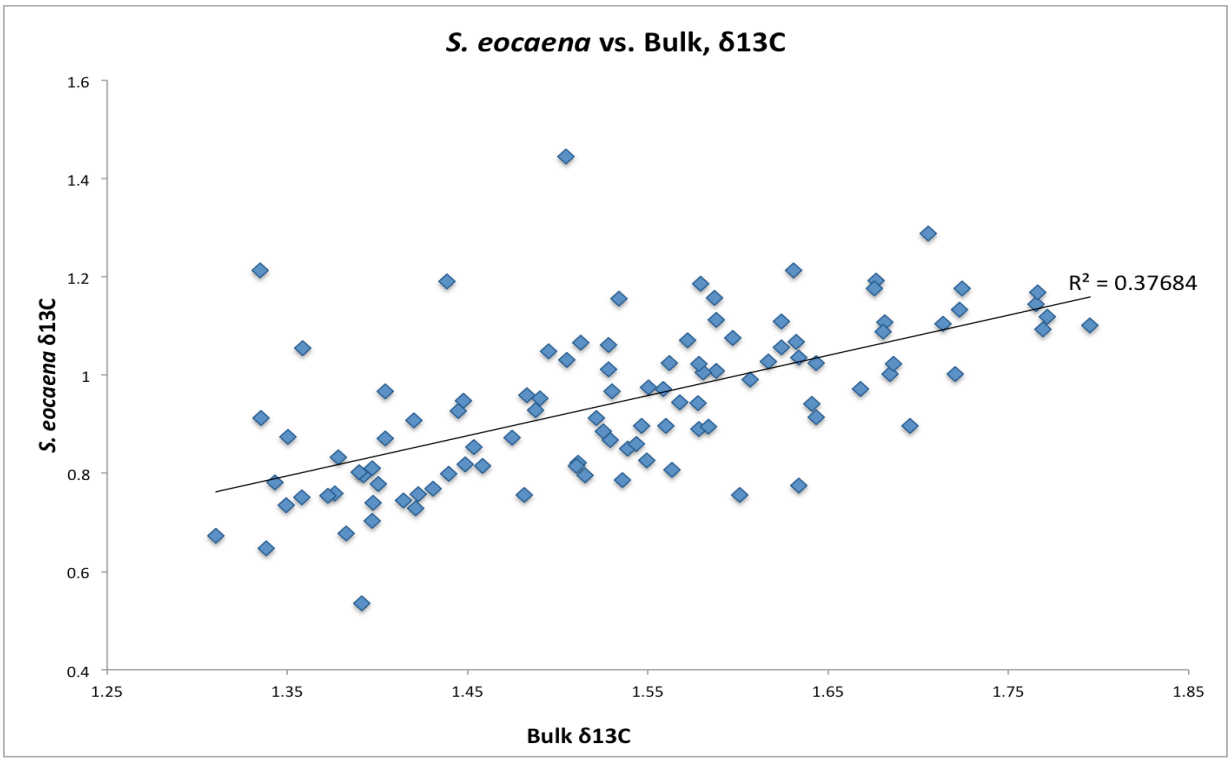

Figure 10. *S. eocaena* $\delta^{13}C$ results plotted against bulk sediment $\delta^{13}C$ results. A linear regression was performed on the dataset and the resulting R^2 value is provided on the chart.

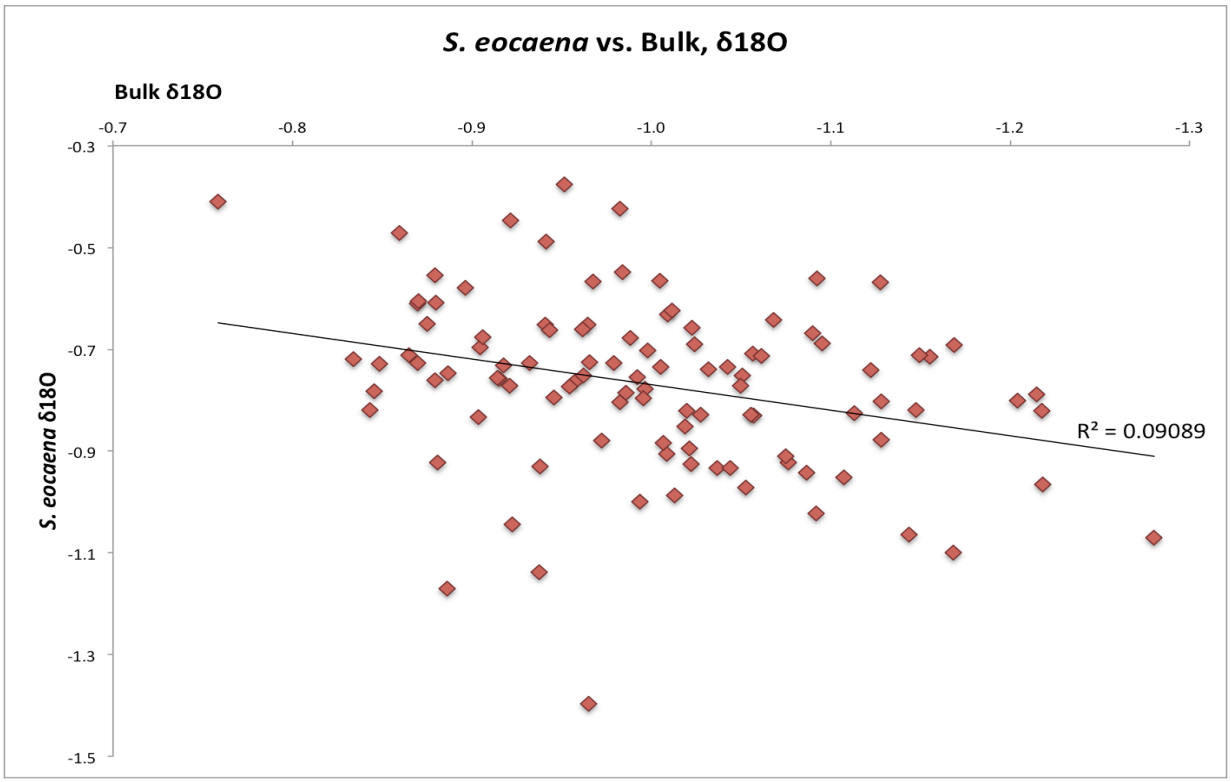

Figure 11. *S. eocaena* $\delta^{18}O$ results plotted against bulk sediment $\delta^{18}O$ results. A linear regression was performed on the dataset and the resulting R^2 value is provided on the chart.

4.3 Spectral Analysis Results

Spectral analysis was performed to determine whether the orbital cyclicity found in the coarse fraction and XRF data is present in any of the foraminiferal stable isotope records. For the spectral analysis, each record was first linearly interpolated to a set resolution of 6 cm to ensure uniform sampling resolution across the dataset (actual study resolution ranged from 6 to 12 cm). The data was then de-trended using a polynomial function before spectral analysis was performed. Figures 12 and 13 show the results of the spectral analysis for $\delta^{13}C$ and $\delta^{18}O$, respectively. Each figure includes results for the *S. eocaena*, *A. bullbrooki*, bulk sediment and *N. trumpeyi* stable isotope records. Two charts are displayed for each record. The top chart shows the power spectrum on a linear scale (Y-axis) plotted against frequency in cycles per meter composite depth (X-axis). The bottom chart shows confidence level estimates, with the dotted red lines representing 90%, 95% and 99% confidence levels. All spectral calculations presented here are based on an estimated sedimentation rate of 3 cm/kyr for the entire study interval.

Figure 12 shows the spectral analysis results for the $\delta^{13}C$ records. All four of these records display a clear peak at the frequency of approximately 1 cycle/m, with confidence levels above 95%. Based on the estimated sedimentation rate of 3 cm/kyr, this suggests that the most powerful cycle in the $\delta^{13}C$ records has a period of approximately 33 kyr. The *A. bullbrooki* and bulk sediment records also produced clear peaks at the frequency of 2 cycles/m, or a period of approximately 16 kyr. This frequency was not as apparent in the *S. eocaena* record (which shows a very broad peak from 2 to 3 cycles/m) or in the *N. trumpeyi* record (which shows peaks around 1.7 and 2.3 cycles/m).

Figure 13 shows the spectral analysis results for the $\delta^{18}O$ records. Unlike the $\delta^{13}C$ records, there are no uniformly present peaks across all four $\delta^{18}O$ records. The bulk sediment and *N. trumpeyi* records show peaks between 0.5 and 0.75 cycles/m, but the significance of these peaks is limited due to the short length of the study, as fewer than 10 cycles would occur at these frequencies across the 400 kyr interval. The only significant peak for the *A. bullbrooki* $\delta^{18}O$ record is too broad (~2.5 to ~4.5 cycles/m) to determine the specific period length, but the peak from ~1 to ~1.5 cycles/m in the *S. eocaena* record indicates a potential cyclicity of approximately 33 to 40 kyr.

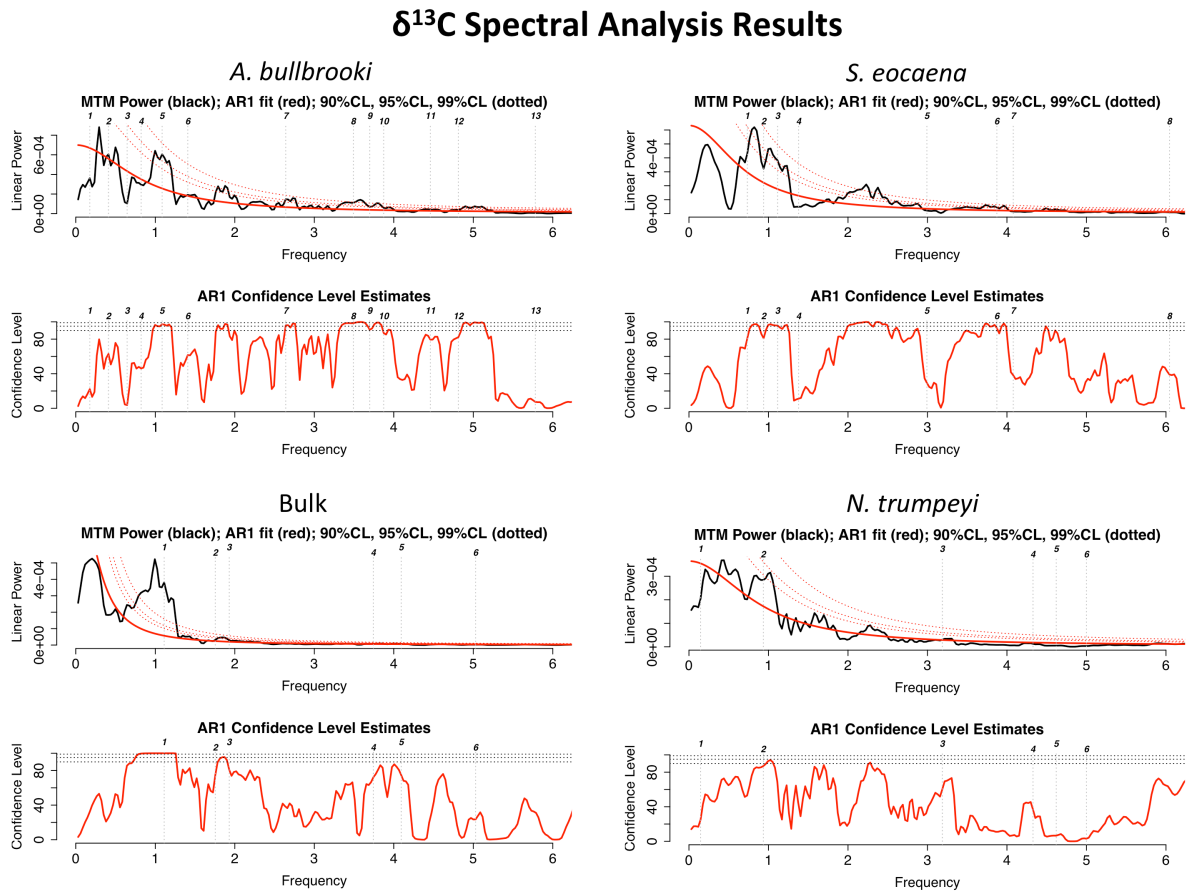

Figure 12. $\delta^{13}C$ spectral analysis results. TOP LEFT: *A. bullbrooki*; TOP RIGHT: *S. eocaena*; BOTTOM LEFT: bulk sediment; BOTTOM RIGHT: *N. trumpeyi*. Upper panels show linear power spectrum (Y-axis) plotted against frequency in cycles/m (X-axis). Lower panels show confidence level estimates, with 90%, 95% and 99% confidence levels denoted by dotted red lines. All analyses were performed on linearly interpolated data with a set resolution of 6 cm.

Several significant limitations should be considered when analyzing these spectral results. Any cycles longer than ~40 kyr should also be approached with caution, as fewer than 10 of these cycles could have occurred across the study interval, thus limiting analytical power. In addition, the age estimates presented here are based on a fixed sedimentation rate of 3 cm/kyr, while the actual sedimentation rate likely varied across the study interval. With these limitations in mind, the most significant finding of this analysis is the peak at 1 cycle/m found in all of the $\delta^{13}C$ records, along with the 2 cycles/m peak found in three of these records. Given the non-uniformity of sedimentation rates across the interval and significant uncertainties associated with the current age model, these cycles are hypothesized to reflect obliquity (~40 kyr) and precession (~23 kyr) orbital cycles. No single frequency is present across all of the the $\delta^{18}O$ records, but the

most significant peaks are also near the 1 cycle/m frequency found in the $\delta^{13}C$ records, thus suggesting that obliquity may be the dominant orbital force for both records.

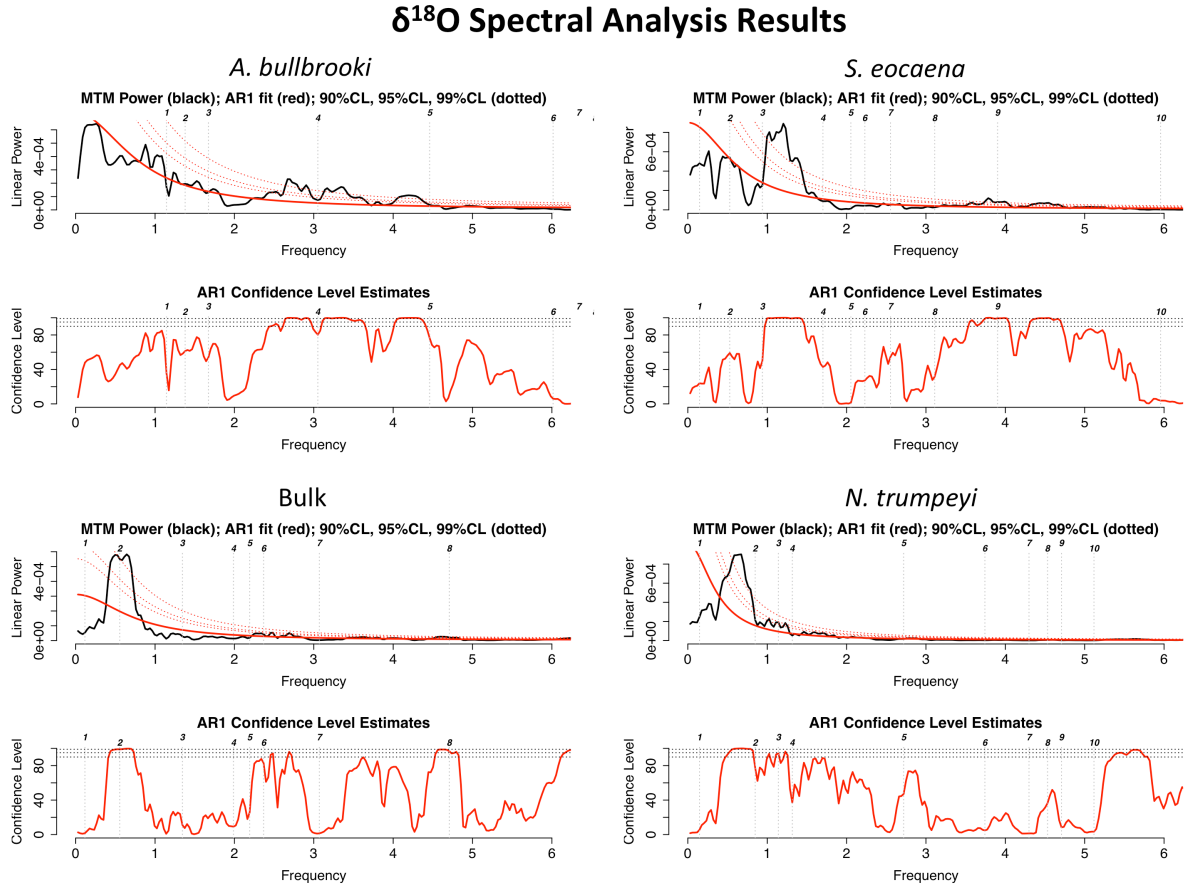

Figure 13. $\delta^{18}O$ spectral analysis results. TOP LEFT: *A. bullbrooki*; TOP RIGHT: *S. eocaena*; BOTTOM LEFT: bulk sediment; BOTTOM RIGHT: *N. trumpeyi*. Upper panels show linear power spectrum (Y-axis) plotted against frequency in cycles/m (X-axis). Lower panels show confidence level estimates, with 90%, 95% and 99% confidence levels denoted by dotted red lines. All analyses were performed on linearly interpolated data with a set resolution of 6 cm.

For comparison with the planktonic records produced in this study, Figure 14 presents spectral analysis results for weight percent coarse fraction (wt % CF) at site 1408 to across the entire C20n magnetochron, spanning an approximate age of 43.4 to 42.3 Ma (Hull *et al.*, 2015). Power (y-axis) is plotted against frequency in cycles/Myr (x-axis) in the image on the right. This longer coarse fraction record produces clear peaks at near orbital frequencies of 30 and 23 kyr. Taking into account the uncertainty of current shipboard age models for this interval, it has been proposed that these peaks correspond to obliquity and precession signals (Hull *et al.*, 2015). The clear cyclicity seen in the coarse fraction record in Figure 2 is therefore confirmed by spectral

analysis. Comparison of the spectral results in Figure 14 with those in Figures 12 and 13 highlights the limitations on analytical precision caused by the short length of our study interval.

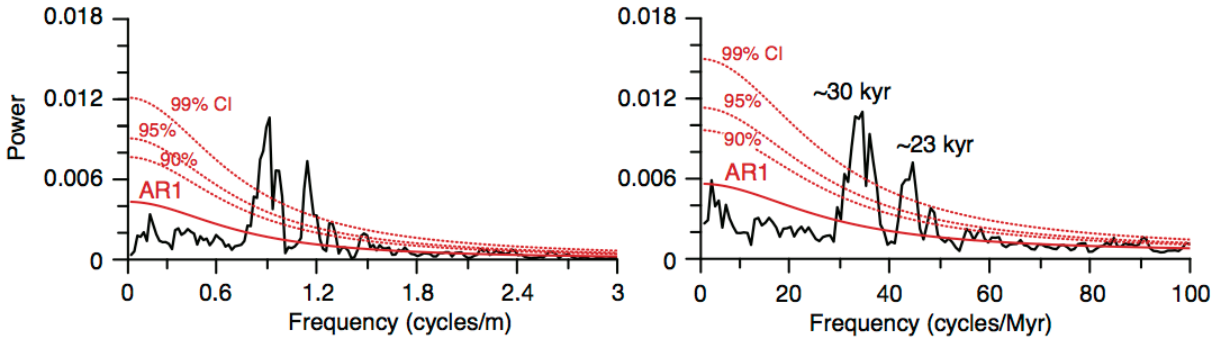

Figure 14. Spectral analysis of wt % CF in the depth (left) and age (right) in magnetochron C20n at 1408 shows significant power at near orbital frequencies. As compared to Figures 12 and 13, spectral analysis over the longer C20n interval produced more precise peaks with reduced background noise. Figure from Hull *et al.* 2015.

4.4 Comparative Results

While the number of comparable high-resolution planktonic foraminiferal stable isotope records from the Eocene is limited, two past studies provide an opportunity for comparison with the results from this study. Edgar *et al.* (2007) produced high resolution (~4.5 kyr) $\delta^{13}C$ and $\delta^{18}O$ records for the planktonic foraminifera *Morozovella lehneri* from an equatorial Atlantic site across an approximately 600 k.y. interval in the Middle Eocene. The benthic foraminifer *Cibicidoides eocaenus* was also used to produce an equivalent benthic record across the study interval. Another useful comparable study was conducted by Burgess *et al.* (2008), in which an extremely high resolution (0.9 kyr) $\delta^{18}O$ record was produced for the planktonic foraminifer *Globigerinatheka index* from a Southern Pacific site across a 70 k.y. window in the <iddle Eocene. This study also produced an equivalent benthic $\delta^{18}O$ record (*Cibicidoides* sp.) for the study interval. Foraminiferal preservation was reported as good to very good for both studies. Comparison of the results from these two studies with the stable isotope records produced in our study enables the placement of our records within the greater context of Eocene ocean variability. This comparison also helps determine the impact of latitude on planktonic foraminiferal stable isotope records, given the large difference in sampling locations between the three studies considered here.

Figure 15 displays the $\delta^{13}C$ records for *A. bullbrooki* and *S. eocaena* produced in this study, alongside the $\delta^{13}C$ record for *M. lehneri* produced by Edgar *et al.* (2007). All of these

datasets have been linearly de-trended. The values presented in Figure 15 represent the residuals from a linear regression performed on each dataset, and the standard deviation values are calculated from these residuals. It is important to note that the Y-axis scales for each dataset are not equivalent. The records from this study span a time interval of approximately 400 kyr, while the Edgar *et al.* study interval is approximately 600 kyr. The $\delta^{13}C$ standard deviations for both planktonic species in this study are lower than the $\delta^{13}C$ standard deviation produced from the Edgar *et al.* (2007) data. This difference is not statistically significant, however, as shown in the test of equal variance results presented in Figure 16.

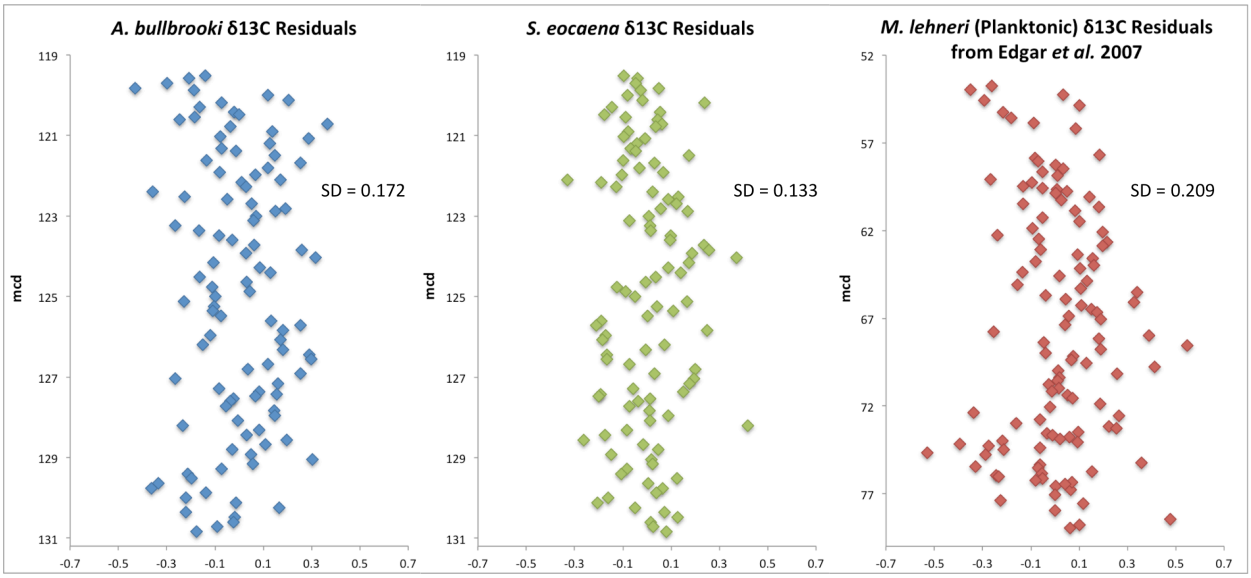

Figure 15. Linearly de-trended $\delta^{13}C$ records for *A. bullbrooki* and *S. eocaena* (this study) plotted alongside the linearly de-trended *Morozovella lehneri* $\delta^{13}C$ record produced by Edgar *et al.* (2007). Standard deviation values are calculated from the de-trended datasets. The X-axis scales are constant throughout the figure, but the Y-axis scales do not convey differences in study interval duration between the datasets.

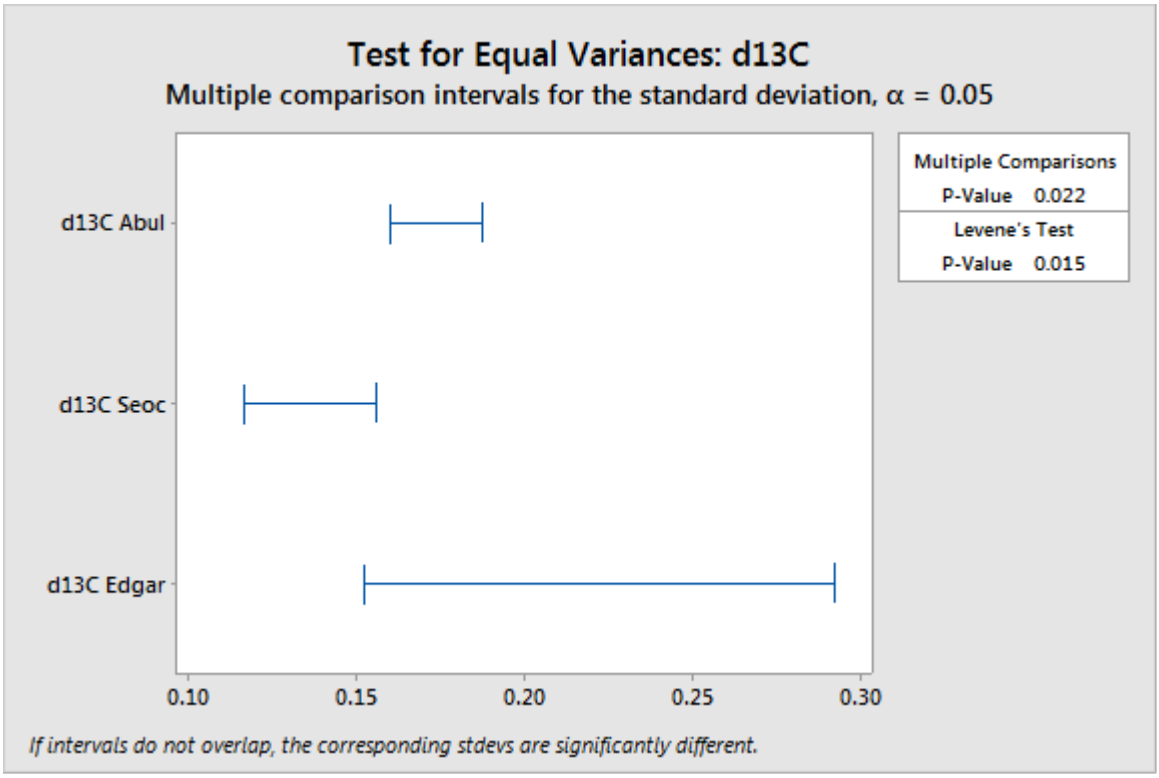

Figure 16. Results of test for equal variances between the linearly de-trended *S. eocaena*, *A. bullbrooki*, and *M. lehneri* (Edgar *et al.* 2007) $\delta^{13}C$ records. The overlapping bars suggest that the standard deviations of this study's datasets are not significantly different from the standard deviation of the *M. lehneri* dataset. Test was conducted using Minitab 17 Statistical Software.

Figure 17 displays the $\delta^{18}O$ records for *A. bullbrooki* and *S. eocaena* produced in this study, alongside the $\delta^{18}O$ record for *M. lehneri* (Edgar *et al.*, 2007) and the $\delta^{18}O$ record produced for *G. index* (Burgess *et al.*, 2008). The $\delta^{18}O$ for *A. bullbrooki* and *S. eocaena* both show higher relative variability than the *M. lehneri* $\delta^{18}O$ record from Edgar *et al.* (2007), but lower variability than the *G. index* $\delta^{18}O$ record from Burgess *et al.* (2008). As shown in Figure 18, the difference in $\delta^{18}O$ standard deviations between this study's records and the Edgar *et al.* (2007) record were not statistically significant, but the Burgess *et al.* (2008) standard deviation was significantly higher than those of the other three studies. Table 2 presents depth habitat, sampling location, time interval, long-term climate and resolution information about each planktonic record used in this comparison, as well as the de-trended standard deviation values calculated for each record.

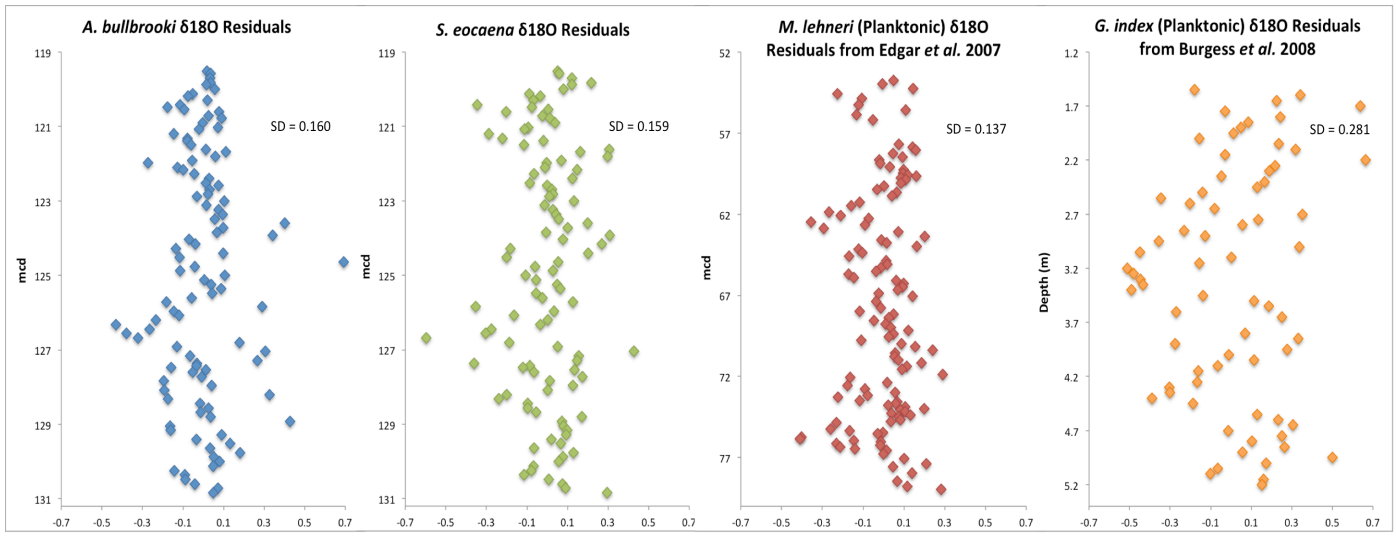

Figure 17. Linearly de-trended $\delta^{18}O$ records for *A. bullbrooki* and *S. eocaena* (this study) plotted alongside the linearly de-trended *Morozovella lehneri* $\delta^{18}O$ record produced by Edgar *et al.* (2007) and the linearly de-trended *Globigerinatheka index* $\delta^{18}O$ record produced by Burgess *et al.* (2008). Standard deviation values are calculated from the de-trended datasets. TheX-axis scales are constant throughout the figure, but the Y-axis scales do not convey differences in study interval duration between the datasets.

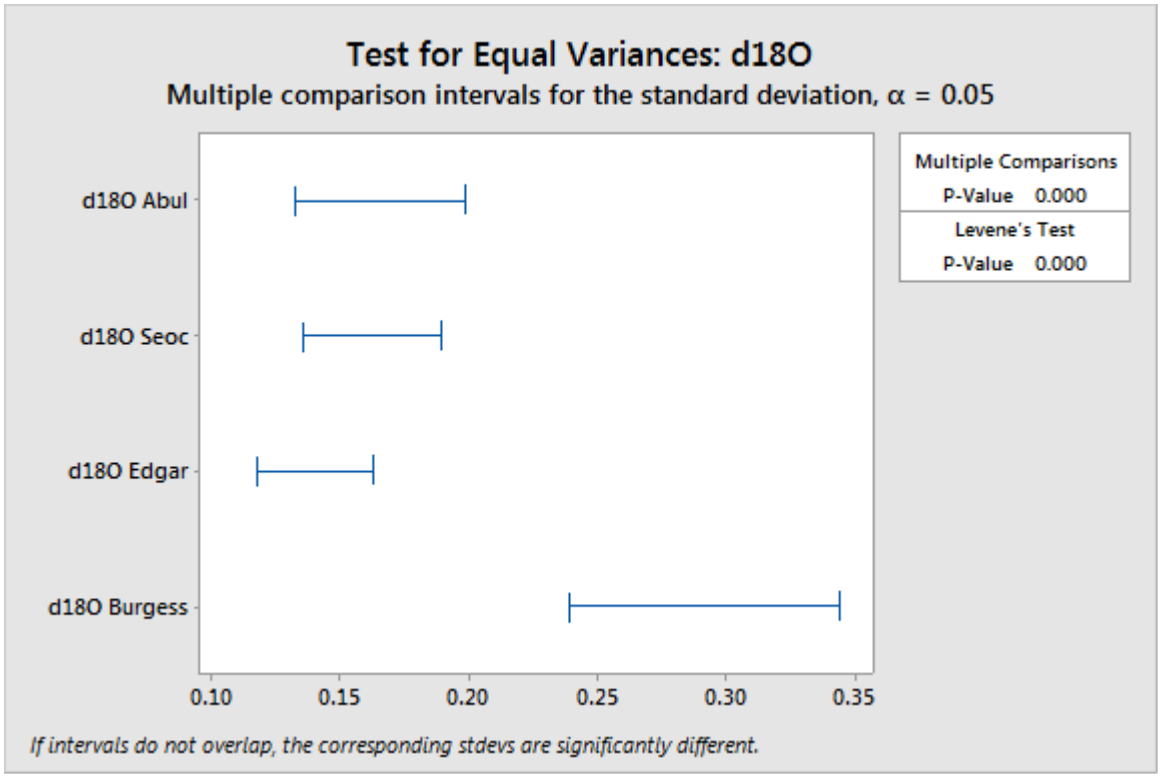

Figure 18. Results of test for equal variances between the linearly de-trended *S. eocaena*, *A. bullbrooki*, *M. lehneri* (Edgar *et al.* 2007) and *G. index* (Burgess *et al.* 2008) $\delta^{18}O$ records. The standard deviations of the records from this study and the Edgar *et al.* (2009) study are not significantly different, but the Burgess *et al.* (2008) study shows significantly higher variability. Test was conducted using Minitab 17 Statistical Software.

	***Acarinina bullbrooki* (this study)**	***Subbotina eocaena* (this study)**	***Morozovella lehneri* (Edgar *et al.* 2007)**	***Globigerinatheka index* (Burgess *et al.* 2008)**
Depth habitat	Surface mixed layer	Thermocline	Surface mixed layer	Surface mixed layer
Location	Northern Atlantic	Northern Atlantic	Equatorial Atlantic	Southern Pacific
Time interval	~42 Ma	~42 Ma	~42 – 41.6 Ma	~41.7 Ma
Climate event	Stable	Stable	Hyperthermal	Stable
Resolution	3-4 kyr	3-4 kyr	~4.5 kyr	0.9 kyr
SD $\delta^{13}C$	0.172	0.133	0.209	
SD $\delta^{18}O$	0.160	0.159	0.137	0.281

Table 2. Relevant information and linearly de-trended standard deviation statistics for the Edgar *et al.* (2007) and Burgess *et al.* (2008) planktonic foraminiferal records, along with equivalent information for the *A. bullbrooki* and *S. eocaena* records produced in this study.

Figure 19 displays the benthic $\delta^{18}O$ records for *N. trumpeyi* (this study), alongside the $\delta^{18}O$ records produced for *C. eocaenus* (Edgar *et al.*, 2007) and *C.* sp. (Burgess *et al.*, 2008). The variability in the benthic $\delta^{18}O$ record from this study is significantly lower than the variability found in the Edgar *et al.* (2007) dataset, but significantly higher than the variability found in the Burgess *et al.* (2008) dataset (as demonstrated in Figure 20). In summary, the variability of the low-latitude Edgar *et al.* (2007) planktonic records did not significantly differ from the variability found in this high-latitude study, while variability of the benthic records differed significantly between all three studies in the comparison.

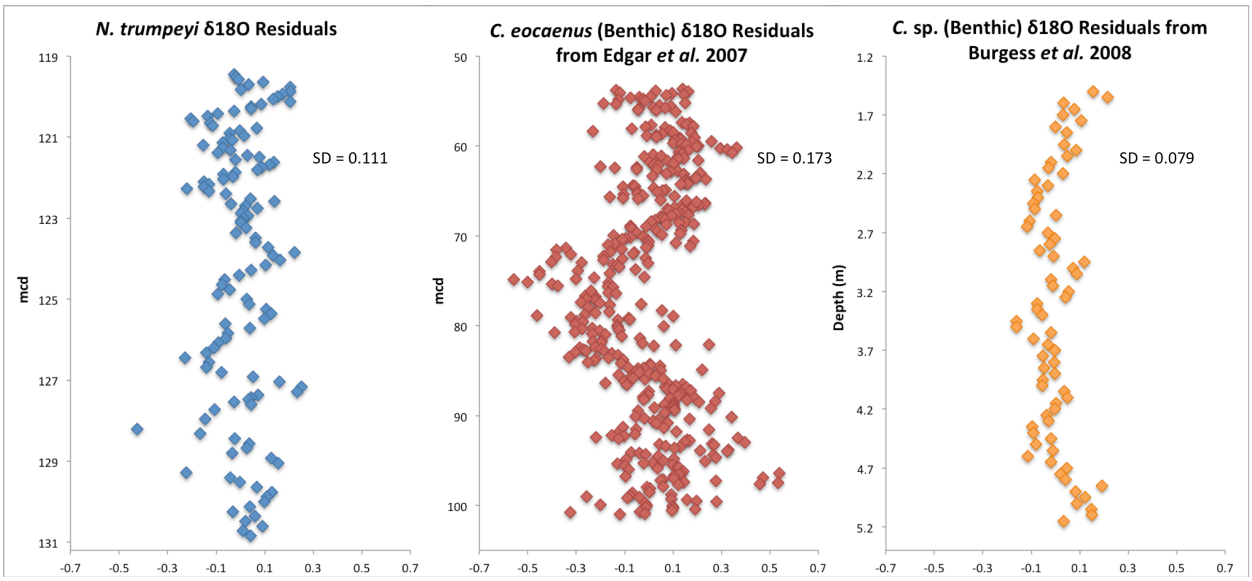

Figure 19. Linearly de-trended $\delta^{18}O$ records for *N. trumpeyi* (benthic, this study) plotted alongside the linearly de-trended *Cibicidoides eocaenus* $\delta^{18}O$ record produced by Edgar *et al.* (2007) and the linearly de-trended *Cibicidoides* sp. $\delta^{18}O$ record

produced by Burgess *et al.* (2008). Standard deviation values are calculated from the de-trended datasets. The X-axis scales are constant throughout the figure, but the Y-axis scales do not convey differences in study interval duration between the datasets.

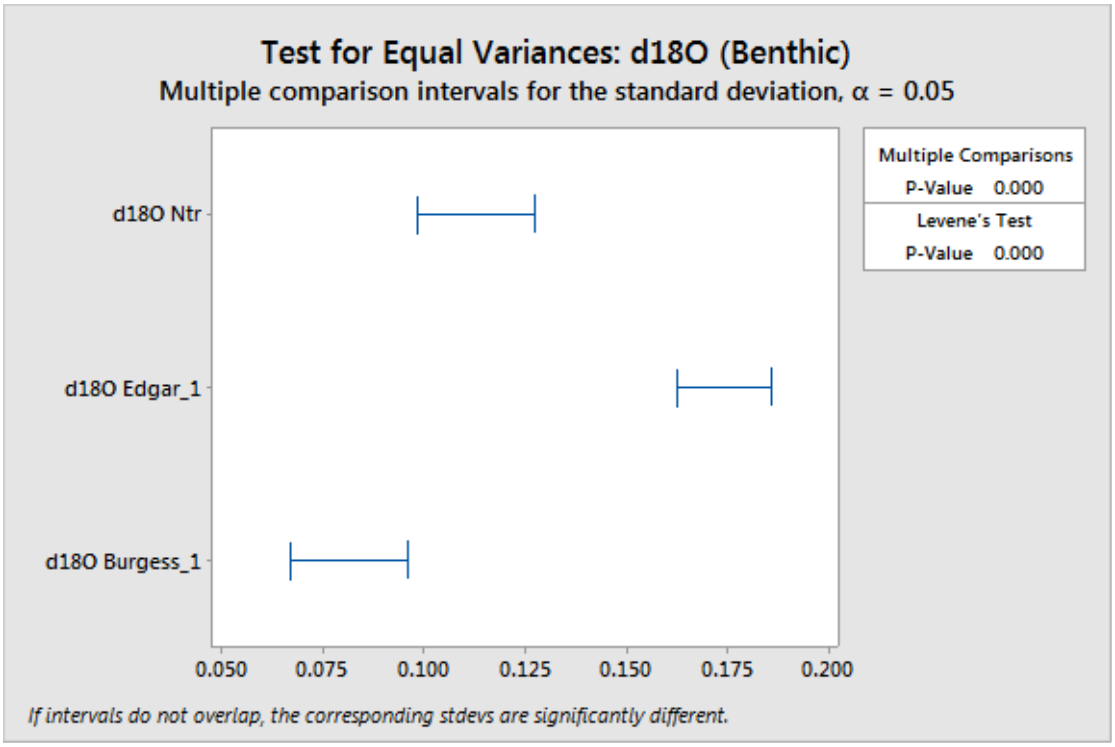

Figure 20. Results of test for equal variances between the linearly de-trended benthic *N. trumpeyi*, *C. eocaenus* (Edgar *et al.* 2007) and *C.* sp. (Burgess *et al.* 2008) $\delta^{18}O$ records. The standard deviations for all three records are significantly different. The *C. eocaenus* record from Edgar *et al.* (2007) shows significantly higher variability than this study's benthic record, while the *C.* sp. record from Burgess *et al.* (2008) shows significantly lower variability. Test was conducted using Minitab 17 Statistical Software.

4.5 Methodological Comparison

As discussed in Sections 1 and 2, two distinct methods were used for data collection in this project. Roughly one third of the planktonic foraminiferal stable isotope measurements in this study (mcd 119.52 to 123.00) were taken from samples of three to five whole specimens (the "2015 methodology"), while the remaining measurements were made on aliquots from samples of around thirty specimens (the "2016 methodology"). Both methods are commonly used in foraminiferal geochemistry research, and this study presents an unprecedented opportunity to identify any discrepancies between the results produced by these methods. Of particular interest is the relative variability found in records produced by these two methods, as this statistic may indicate relative levels of analytical precision. Figure 21 shows the planktonic $\delta^{13}C$ and $\delta^{18}O$ records produced in this study via the two distinct methods. The lighter data points represent all of the duplicate and triplicate measurements made using the 2015 methodology (all other

analyses in this paper have used the average values of these multiple measurements), while the darker data points represent measurements made using the 2016 methodology.

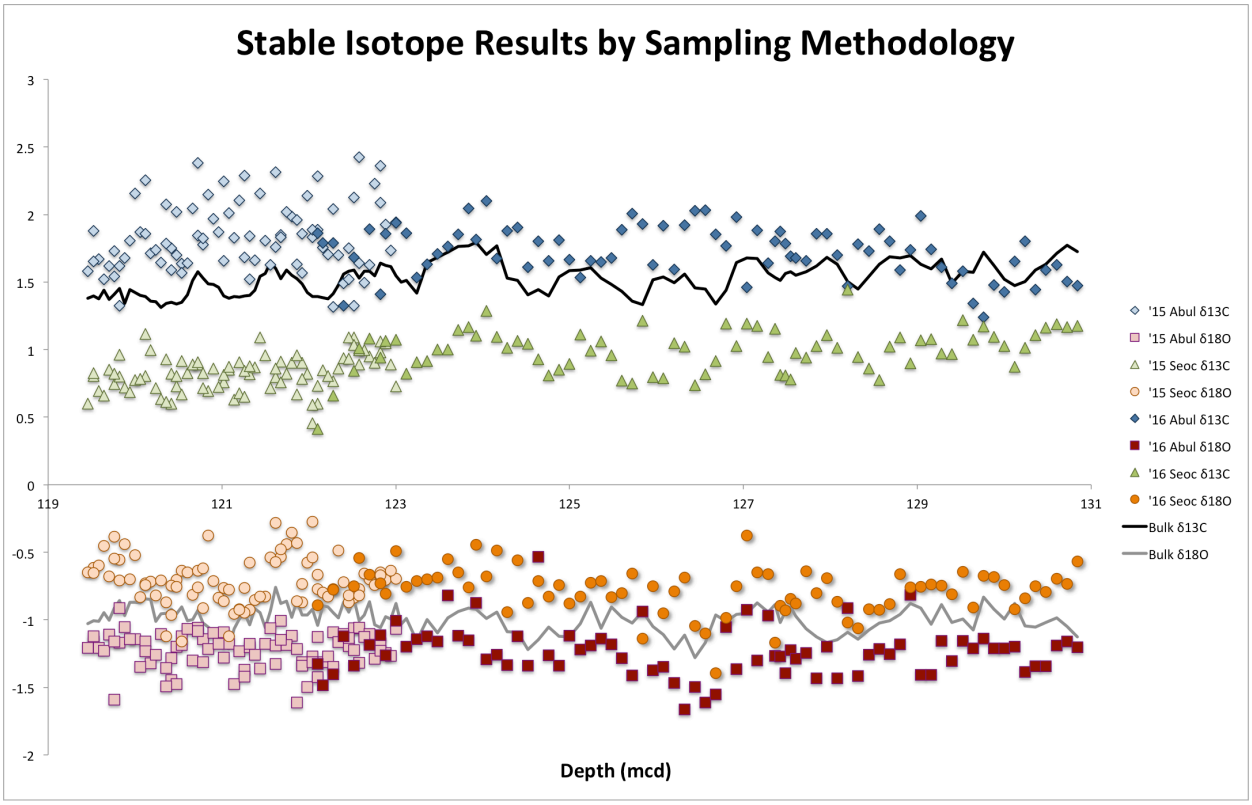

Figure 21. Planktonic δ13C and δ18O records by sampling methodology. Lighter data points represent measurements (including duplicates and triplicates) collected using the 2015 methodology (3-5 individual specimens per measurement), while darker data points represent measurements collected using the 2016 methodology (aliquots from 30 crushed specimens).

A preliminary visual analysis of Figure 21 suggests that the variability of the records produced by the two sampling methods is very similar, with the exception of the *A. bullbrooki* $\delta^{13}C$ record, for which the 2015 methodology produced significantly higher variability. Another significant observation is the apparent offset between the two methodologies in the *S. eocaena* $\delta^{13}C$ record, which could be an artifact of the difference in sampling technique. A more quantitative comparison of the two methodologies is presented in Figure 22 and in Tables 3 and 4. Figure 22 displays the residuals of linear regressions that were performed each separate dataset, along with standard deviation values calculated from these residuals. Tables 3 and 4 present the calculated standard deviation values for the de-trended $\delta^{13}C$ and $\delta^{18}O$ records, respectively. For the *A. bullbrooki* $\delta^{13}C$ record, the standard deviation for the 2015 methodology was significantly higher than for the 2016 methodology. For the *S. eocaena* $\delta^{13}C$ record, the variability was not significantly different between the two methodologies. The variability of the

A. bulbrooki $\delta^{18}O$ record was significantly higher when the 2016 methodology was used, while the variability of the *S. eocaena* $\delta^{18}O$ record was slightly lower with the 2016 methodology.

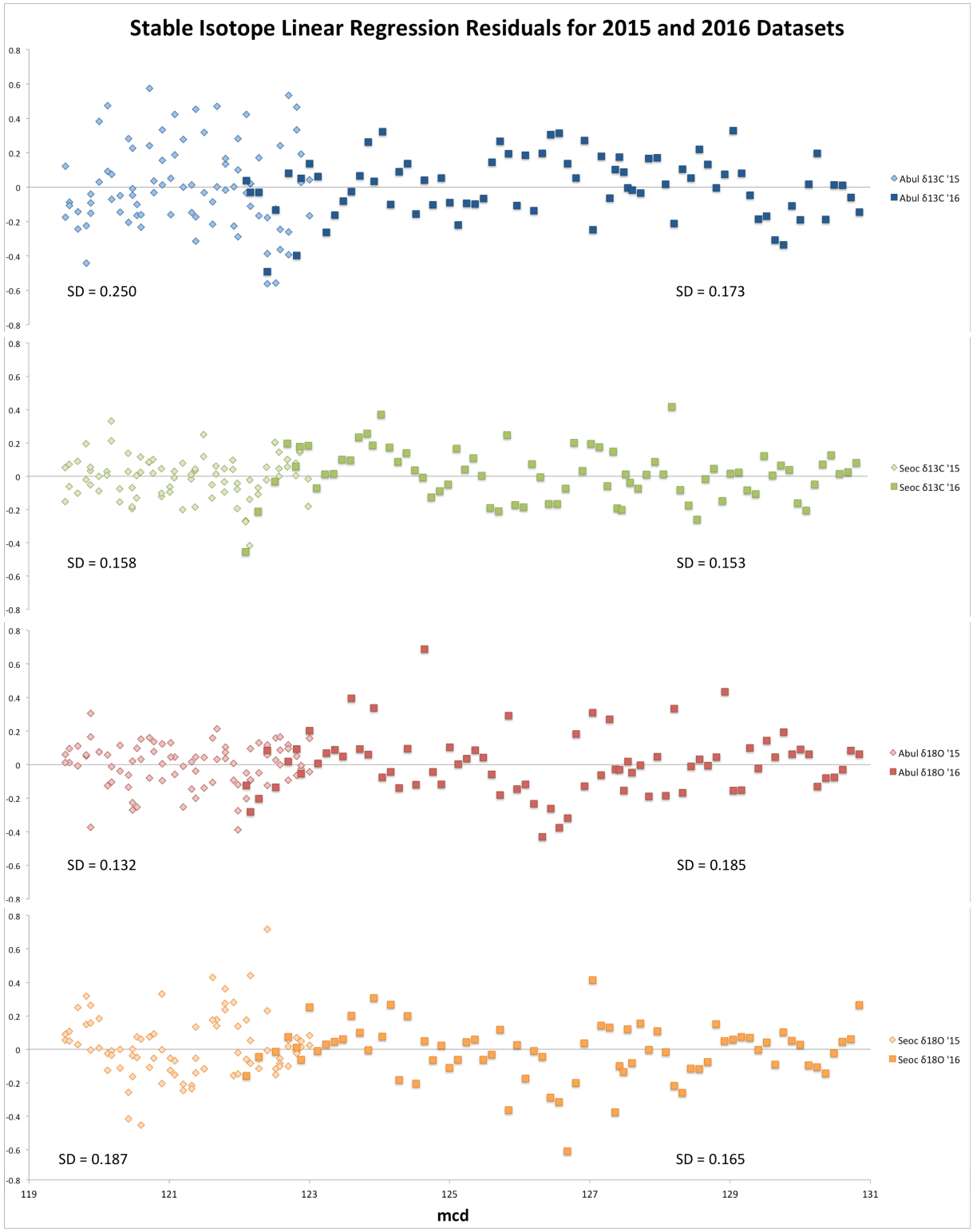

Figure 22. Linear regression residuals of planktonic δ13C and δ18O records. Lighter data points represent measurements (including duplicates and triplicates) collected using the 2015 methodology, while darker data points represent measurements

collected using the 2016 methodology. Regressions were performed separately on each dataset, and standard deviation values are calculated from residuals.

Record	Standard Deviation 2015 Methodology Duplicate Samples	Standard Deviation 2015 Methodology Averages	Standard Deviation 2016 Methodology
A. bullbrooki $\delta^{13}C$	0.250	0.189	0.173
S. eocaena $\delta^{13}C$	0.158	0.109	0.153

Table 3. Standard deviation values calculated from linear regression residuals of $\delta^{13}C$ datasets, separated by methodology.

Record	Standard Deviation 2015 Methodology Duplicate Samples	Standard Deviation 2015 Methodology Averages	Standard Deviation 2016 Methodology
A. bullbrooki $\delta^{18}O$	0.132	0.084	0.185
S. eocaena $\delta^{18}O$	0.187	0.142	0.165

Table 4. Standard deviation values calculated from linear regression residuals of $\delta^{18}O$ datasets, separated by methodology.

Tables 3 and 4 present the standard deviation values calculated from the linearly de-trended planktonic $\delta^{13}C$ and $\delta^{18}O$ records, separated by methodology. In these tables, standard deviations were also calculated for the datasets produced by averaging the duplicate and triplicate measurements made using the 2015 methodology (these datasets have been used in all other analyses in this paper). When this averaging technique is performed, the 2015 methodology produces significantly lower variability than the 2016 methodology for all records except the *A. bullbrooki* $\delta^{13}C$ record. While no uniform difference in variability is apparent between the two methodologies when only individual measurements are considered, it appears that averages of multiple measurements of 3 to 5 individual specimens may produce lower variability than single measurements of aliquots from samples of 30 crushed specimens.

5. Discussion

5.1 Stable Isotope Records: Variability and Orbital Cyclicity

The congruence between this study's planktonic foraminiferal stable isotope records and the orbital-forced cyclicity in the coarse fraction and XRF records is limited. The coarse fraction and XRF Ca/Al records both show 11 clear peak-and-trough cycles across the study interval. These cycles are hypothesized to represent the obliquity signal (~40 kyr), given the roughly 400

kyr length of the study interval. This study spans a sedimentary interval of approximately 11 meters, so the corresponding obliquity signal was expected to appear in the planktonic records at a frequency of about 1 cycle per meter. As is shown in Figure 12, this peak appears in both planktonic $\delta^{13}C$ records, along with the bulk and benthic records, with a confidence level above 90%. In the *A. bullbrooki* $\delta^{13}C$ record, this peak appears alongside four additional higher-frequency peaks. In the *S. eocaena* record, the obliquity peak is extremely broad (spanning from ~0.5 to ~1.5 cycles/m), and several broad higher-frequency peaks are also present. The prominence of these broad, high-frequency peaks suggests that the obliquity signal in both planktonic $\delta^{13}C$ records is obscured by significant background noise (random variation). Nonetheless, evidence is still present for the dominance of orbital forcing at the 1 cycle/m frequency in the $\delta^{13}C$ records. This interpretation is also supported by visual analysis of the records presented in Figure 2.

Even more striking is the lack of significant orbital cyclicity in our $\delta^{18}O$ records. The *A. bullbrooki* $\delta^{18}O$ record does not produce a significant peak near 1 cycle/m, and the obliquity peak in the *S. eocaena* $\delta^{18}O$ records is extremely broad. The lack of precise low-frequency peaks and the prominence of broad high-frequency peaks in the planktonic $\delta^{18}O$ records suggest either an absence of orbital-scale cyclicity across the study interval, or that any orbital signals are obscured by random variability. Visual analysis of the $\delta^{18}O$ records also suggests random intra-species variability with no obvious cyclic patterns. This intra-species variability is not thought to reflect $\delta^{18}O$ variability between individual foraminifera (e.g. seasonality) because large sample sizes were used throughout the study. These results therefore suggest significant random, non-cyclic $\delta^{18}O$ variability at the population level.

The lack of orbital-scale cyclicity in the planktonic $\delta^{18}O$ records and the incongruity between the $\delta^{13}C$ and $\delta^{18}O$ records is surprising, and several possible interpretations are possible. The first explanation hypothesizes that the planktonic foraminifera are actively engaged in "habitat tracking," moving through the water column in direct response to temperature changes. This temperature-induced migration would be expected to obscure any orbital patterns in the $\delta^{18}O$ record, as the foraminifera would be following relatively constant $\delta^{18}O$ DIC conditions. If $\delta^{13}C$ DIC was changing in relation to $\delta^{18}O$ DIC over orbital timescales during the Eocene, this could produce the cyclic patterns that appear in this study's carbon isotope records. The habitat tracking interpretation must take into account the fact that *A. bullbrooki* is generally believed to

be an obligate symbiont-bearer, which if true would greatly restrict its potential vertical range due to light requirements (Norris *et al.*, 1996; Birch *et al.*, 2012).

This study's results could also be explained without the assumption of habitat tracking. If the planktonic foraminifera are assumed to remain at constant depth habitats (or are moving randomly with regard to water column depth), the carbon-oxygen discrepancy observed here could simply be the result of a difference in the relative magnitude of $\delta^{18}O$ DIC versus $\delta^{13}C$ DIC variability over orbital timescales. Smaller changes in $\delta^{18}O$ DIC could be obscured by background, intraspecific variability (e.g. intraspecific depth habitat heterogeneity or seasonality effects), while the larger $\delta^{13}C$ DIC variability would still appear in the planktonic records. This explanation is weakened by the fact that depth habitat heterogeneity and seasonality effects would most likely be obscured by the large sample sizes used in this study.

It has also been suggested that global sea surface temperature (SST) sensitivity to radiative forcing may be strongly influenced by sea ice albedo processes, especially over millennial timescales (Rohling *et al.*, 2012). Most Cenozoic paleoclimate reconstructions (largely based on benthic foraminiferal $\delta^{18}O$) suggest that the Eocene epoch was largely ice-free (Zachos *et al.*, 2001; Pearson *et al.*, 2007; Burgess *et al.*, 2008). It is therefore possible that surface water temperatures at our high-latitude sample site were not sensitive to orbital-forced radiative change, and thus our non-cyclic planktonic $\delta^{18}O$ records are the result of SST stability across the study interval. This explanation fails, however, to account for the obliquity signal apparent in our planktonic $\delta^{13}C$ records and the orbital-scale $\delta^{18}O$ variability found in the benthic records.

All three of these proposed explanations also fail to address the fact that the variability of our planktonic $\delta^{13}C$ records, while more coherent along orbital frequencies, is not of significantly greater magnitude than the variability of our planktonic $\delta^{18}O$ records. The standard deviation values presented in Table 1 demonstrate that $\delta^{18}O$ variability is either similar to or greater than $\delta^{13}C$ variability (0.160 vs. 0.172 for *A. bullbrooki*; 0.159 vs. 0.133 for *S. eocaena*, respectively). If the habitat tracking hypothesis is assumed, the expected $\delta^{18}O$ variability should be significantly lower than the expected $\delta^{13}C$ variability, as the foraminifera would be following relatively constant temperature conditions. Likewise, the second and third explanations presented above both propose that $\delta^{13}C$ orbital-forced variability must be larger than $\delta^{18}O$ variability. The variability of our $\delta^{18}O$ records is less coherent and more random, but is not smaller in magnitude

than the variability of our $\delta^{13}C$ records. It is important to note, however, that background variability is also present in the $\delta^{13}C$ records. The obliquity signal in our planktonic $\delta^{13}C$ records is obscured by significant background noise, as is clear in a comparison of the spectral results presented in Figure 12 (our $\delta^{13}C$ records) and Figure 14 (coarse fraction data for the entire C20n magnetochron).

With these limitations in mind, several tentative conclusions can be drawn from our results. First, the variability of our $\delta^{18}O$ records suggests that planktonic foraminifera do not actively engage in "habitat tracking" over millennial timescales. Second, the clear obliquity signal in our planktonic $\delta^{13}C$ records indicates the presence of orbital forcing of surface ocean characteristics across the study interval. With this in mind, the strongest explanation for the discrepancy between our planktonic $\delta^{13}C$ and $\delta^{18}O$ records is that orbital-forced $\delta^{13}C$ DIC variability was of greater magnitude than $\delta^{18}O$ DIC variability, and thus background variability only obscured the smaller obliquity signal in the $\delta^{18}O$ records. This conclusion is extremely tentative, and several questions remain. In particular, the similarity in the magnitude of $\delta^{13}C$ and $\delta^{18}O$ variability weakens all of the proposed explanations for our results, and future work should focus on determining the relative importance of environmental versus biological and ecological effects in producing these unexpected patterns.

The addition of Mg/Ca measurements, for which 28 samples across the study interval have already been prepared, will provide more certain temperature estimates. This data will help determine whether the variability in our planktonic $\delta^{18}O$ records is indeed reflecting random temperature or depth habitat changes across the study interval. Foraminiferal $\delta^{18}O$ values can be influenced by seawater carbonate ion concentration, pH and salinity, while Mg/Ca provides more direct information about seawater temperature (Pearson *et al.*, 2012; Elderfield *et al.*, 2002). If the Mg/Ca results suggest that the planktonic foraminifera are experiencing non-cyclic, high-magnitude temperature variability, it will be difficult to explain why more coherent orbital-scale cyclicity is found in the $\delta^{13}C$ record given our current understanding of planktonic foraminiferal ecology and test geochemistry.

5.2 Stable Isotope Records: Planktonic-Benthic Decoupling

Another unexpected finding of this study, as shown in Figure 13, is the lack of congruity between the planktonic and benthic $\delta^{18}O$ records. The *N. trumpeyi* record produces a significant

peak between 0.5 and 1 cycle/m, while the *A. bullbrooki* record produces no significant peaks below 2.5 cycles/m and the *S. eocaena* record produces a peak between 1 and 1.5 cycles/m. It appears that, during greenhouse conditions and at high latitudes, planktonic and benthic stable isotope records do not provide the same information over orbital timescales. One of the most significant and important paleoceanographic challenges is the tracking of past surface ocean dynamics, as the surface ocean is thought to better represent the geologic processes of weathering and deposition, and surface to deep ocean gradients are essential for deciphering oceanic processes (Hilting *et al.*, 2008; Kump, 1991). The discrepancy between this study's stable isotope records suggests that either planktonic foraminifera or benthic foraminifera (or both) are not reliable indicators of surface ocean characteristics on millennial timescales.

This discrepancy was particularly surprising given the high-latitude location of the study site, as North Atlantic deep-water formation would be expected to create a strong link between planktonic and benthic temperature ($\delta^{18}O$) patterns (Broecker, 1991). The planktonic-benthic decoupling found in this study could be explained, however, by reduced North Atlantic deep-water formation during the greenhouse conditions of the Eocene (as hypothesized by Via & Thomas (2006), who suggest that significant North Atlantic deep-water circulation did not begin until the early Oligocene). If orbital-forced surface ocean temperature change during the Middle Eocene was minimal, as suggested by our planktonic $\delta^{18}O$ records, the cyclic patterns found in our benthic $\delta^{18}O$ record could reflect orbital-forced changes in deep-water sourcing. It is possible that Eocene North Atlantic deep-water was sourced locally under certain orbital configurations, while sourced non-locally (from the Southern Hemisphere, for example) during others. This pattern could have produced the cyclic changes in seawater $\delta^{18}O$ which are reflected in our benthic record.

A related explanation for the lack of correlation between sediment and benthic signals and our planktonic foraminiferal records rests on the fact that Site U1408 is a sediment drifts site (Norris *et al.*, 2014). The strong XRF Ca/Al and coarse fraction cyclicity patterns may be the result of orbital-forced changes in bottom water current velocities (i.e. high current velocities caused sediment winnowing during coarse fraction peaks). Such orbital-forced drift patterns may not have impacted surface water environments, and thus would not have appeared in the planktonic foraminiferal records. These two related explanations suggest that orbital-scale changes in deep ocean circulation patterns (both global and local) could be responsible for the

discrepancies between our planktonic and benthic stable isotope records. As described above, foraminiferal $\delta^{18}O$ values can be influenced by seawater carbonate ion concentration, pH and salinity, and changes in deep-water sourcing could impact benthic $\delta^{18}O$ through these factors. The addition of benthic Mg/Ca data will provide more definite deep-water temperature estimates and will help determine the relative significance of temperature versus deep-water sourcing in producing the patterns seen in our benthic $\delta^{18}O$ record.

5.3 Effects of Latitude: Comparison with Equatorial Atlantic Records

To place this study within the greater context of Eocene paleoceanography, our stable isotope records are compared to similar records produced by Edgar *et al.* (2007). The most surprising finding was the apparently minimal effect of latitude on planktonic foraminiferal stable isotopes. The variability of our high-latitude $\delta^{13}C$ and $\delta^{18}O$ records was not significantly different than the variability found at the equatorial Atlantic site studied by Edgar *et al*., as shown in Figures 15 through 18 and Table 2. This is surprising because latitude would be expected to have a significant impact on the magnitude of orbital-forced changes in temperature, productivity and biological pump efficiency in the upper water column (Rohling *et al.*, 2012).

The minimal effects of latitude on middle Eocene planktonic foraminiferal stable isotope records might be explained by the generally weaker impact of orbital-forced climatic variation on surface ocean characteristics during the ice-free Eocene (Zachos *et al.*, 2001). This explanation is brought into question, however, by the presence of extremely clear obliquity signals in other datasets such as XRF productivity proxies across our study interval.

It is also possible that the unexpected results of this comparison are due to differences in long-term climate trends between the two studies. Our study presents the first Eocene high-resolution planktonic stable isotope records from a period of long-term climate stability, so no comparable records exist to facilitate a latitudinal comparison without the potential bias of long-term climate differences. The Edgar *et al.* (2007) study interval encompasses a pronounced and abrupt global warming event (most evident in the benthic $\delta^{18}O$ record presented in Figure 19). Differences in long-term climate conditions may have therefore prevented an accurate comparison of high- and low-latitude orbital-scale variability. While this hyperthermal event appears clearly in the Edgar *et al.* (2007) benthic $\delta^{18}O$ record (Figure 19), it is not as apparent in the planktonic stable isotope records (Figures 16 and 17). The planktonic stable isotope records

produced by Edgar *et al.* (2007) actually show remarkably similar variability to our planktonic records, despite large differences in latitude and long-term climate trends.

The minimal impact of latitude and long-term climate on planktonic foraminiferal stable isotopes may shed light on the ability of these organisms to track surface ocean temperature and carbon chemistry over orbital timescales. Latitude and long-term climate appear to have a much stronger effect on benthic $\delta^{18}O$ records, as shown in Figure 19. The fact that these differences do not appear in the planktonic records suggest that biological or ecological effects may be buffering or obscuring environmental signals in the planktonic isotopes. This interpretation is further supported by the lack of orbital cyclicity in the planktonic $\delta^{18}O$ records. Taken together, the results of this study suggest that planktonic foraminiferal stable isotopes may not be reliable indicators of environmental change over orbital timescales.

5.4 Methodology Comparison

As is shown in Figures 20 and 21 and Tables 3 and 4, there are no uniform discrepancies between the results produced via the two sampling methods employed in this study. The aliquot (2016) method produced lower variability on average than the 2015 method, in which measurements were made on 3 to 5 whole specimens. This difference is not uniform across all of the planktonic records, however, as the *A. bullbrooki* $\delta^{18}O$ record shows the opposite trend. The most significant difference between the two methods is found in the *A. bullbrooki* $\delta^{13}C$ record, for which the 2015 method produced much higher variability. This suggests that the surface-dwelling *A. bullbrooki* may have greater $\delta^{13}C$ variability between individual foraminifera than the thermocline-dwelling *S. eocaena*, but this difference is not present in the $\delta^{18}O$ records. It is worth noting, however, that variability was minimized when records were composed of averages of duplicate and triplicate measurements made using the 2015 method. This suggests that measuring (and averaging) multiple small samples may be the most effective means of reducing background variability in planktonic foraminiferal stable isotope records.

5.5 Limitations and Suggestions for Future Work

Several potential limitations should be considered when interpreting the results of this study. First, it has been clearly demonstrated that the preservation of planktonic foraminifera can strongly impact our ability to extract meaningful stable isotope records from foraminiferal calcite

(Sexton *et al*., 2006). The scanning electron microscope images presented in Figure 1 show good preservation with minimal diagenetic calcite, but additional SEM images should be acquired throughout the study interval to confirm the maintenance of these conditions. The instability of the stable isotope gradients between *A. bullbrooki* and the bulk sediment record, as shown in Figure 4, suggests an increase in diagenetic alteration for this species during the earlier portions of the study interval. As noted in Section 4.1, *A. bullbrooki* preservation was noticeably poor across a series of six samples (mcd 125.96 to 126.56). None of these samples, however, produced anomalous stable isotope measurements, suggesting that preservation did not significantly impact our stable isotope results.

Taxonomic error could also impact our stable isotope records, as species-specific biological effects are known to influence planktonic foraminiferal stable isotopes, especially $\delta^{13}C$ (D'Hondt *et al.*, 1994; Friedrich *et al.*, 2012; Birch *et al.*, 2013). *A. bullbrooki* specimens were selected with a high degree of confidence, but *S. eocaena* identifications were less certain due to morphological plasticity within the *Subbotina* genus (Pearson *et al.*, 1993). This uncertainty is not believed to have significantly impacted our results, however, because stable isotope values tend to be highly conserved across the *Subbotina* genus (Breen, 2016).

The short length of the study interval limits the utility of our spectral analysis results. Only 11 obliquity cycles occur across the interval, thus limiting the specificity of the obliquity-forced spectral peaks, as is evident in Figures 12 and 13 (as compared to the more precise peaks from the longer interval presented in Figure 14). While the obliquity signal was still identifiable in our $\delta^{13}C$ records, a longer study interval would enable a more precise analysis and would be especially useful for identifying potential signals in the $\delta^{18}O$ records that may be hidden in part due to our short study interval. The extension of this study interval, or combination with other high resolution planktonic records from the same location, will strengthen the tentative spectral interpretation presented here. In addition, stable isotope data for spectral analysis was linearly interpolated to a resolution of 6 cm, while actual sampling resolution ranged from 6 to 12 cm. The reliability and precision of our spectral results could be improved by collecting stable isotope data at a resolution of 6 cm across the interval, thus eliminating the need for linear interpolation.

Stable isotope measurements for this study were obtained from two separate laboratories (the Yale Analytical and Stable Isotope Center and the University of California, Santa Cruz

Stable Isotope Laboratory). The location of measurement for each sample can be found in Table 5 in the Appendix, and Figure 23 in the Appendix displays our stable isotope results segregated by measurement location. No significant discrepancies are apparent between the two locations, and both laboratories used the same equipment (Kiel IV Carbonate Device with a Thermo MAT 253 isotope ratio mass spectrometer), so this factor is not thought to have influenced the validity of our results.

Two distinct sample preparation methods were also used; 79 of the samples were cleaned by ultrasonication, while 28 samples were cleaned for trace metal analysis (as described in Section 3.1). The sample preparation method for each sample can be found in Table 5 in the Appendix, and Figure 24 in the Appendix displays our stable isotope results segregated by cleaning method. No significant discrepancies are apparent between the two methods. As described in Sections 5.1 and 5.2, the addition of planktonic and benthic Mg/Ca data will provide more definitive temperature estimates across the study interval, thus helping to answer remaining questions surrounding habitat tracking and orbital-forced temperature variation.

In addition to the collection of Mg/Ca data, work is currently being conducted to model expected surface and deep ocean environmental dynamics across our study interval. The largest uncertainty produced by our results is the extent to which biological and ecological effects may be buffering environmental signals in our planktonic stable isotope records. These models will provide information on expected orbital-scale patterns in sea surface temperature and ocean chemistry during the Middle Eocene. Such efforts will be particularly useful in the comparison of our stable isotope records with the low-latitude records produced by Edgar *et al.* (2007), as the models will help determine the expected impact of latitude on environmental conditions and thus the extent to which the planktonic foraminiferal records capture these expected differences. As described in Sections 5.1 through 5.3, the unexpected nature of our planktonic stable isotope records raises the question of whether our results reflect unexpected environmental conditions, the buffering of environmental signals by biological and ecological effects, or some combination of both.

6. Conclusions

The calcium carbonate test geochemistry of planktonic foraminifera is an important paleoceanographic tool, and this study investigates the utility of this tool for tracking

environmental change over millennial timescales during the ice-free Eocene. Our results generally suggest that biological and ecological effects may buffer orbital-scale environmental signals in planktonic foraminiferal stable isotope records. Several tentative conclusions can be drawn from our data, but significant uncertainties remain.

One unexpected finding of this study is the discrepancy between planktonic foraminiferal $\delta^{18}O$ and $\delta^{13}C$ records across the study interval. A clear obliquity (~40 kyr) signal is present in our $\delta^{13}C$ records, but no orbital cyclicity is apparent in the $\delta^{18}O$ data. Greater orbital-scale $\delta^{13}C$ DIC variability (as compared to $\delta^{18}O$ DIC) could explain this discrepancy, and significant random variability in the $\delta^{18}O$ records suggests that planktonic foraminifera do not engage in habitat tracking over millennial timescales. The similarity in magnitude of planktonic $\delta^{13}C$ and $\delta^{18}O$ variability remains difficult to explain, and the addition of planktonic Mg/Ca data will help provide more definitive temperature estimates across the study interval.

A second unexpected finding is the lack of congruity between our planktonic and benthic $\delta^{18}O$ records. Spectral analysis results suggest decoupling of any orbital-scale cyclic $\delta^{18}O$ patterns found in these records. This discrepancy might be explained by orbital-forced changes in deep-water sourcing or bottom current velocities at our high-latitude sampling site. This explanation calls into question the utility of benthic foraminiferal stable isotopes for tracking surface ocean dynamics, although significant questions still remain about the utility of planktonic stable isotopes with regards to this purpose as well.

In particular, the apparently minimal effect of latitude on Eocene planktonic stable isotope records raises concerns about the ability of these organisms to record orbital-scale environmental change. Our high-latitude planktonic records show very similar variability to records produced by Edgar *et al.* (2007) from a low-latitude, equatorial Atlantic sampling site. Latitude is expected to have a significant impact on surface ocean dynamics, with higher-latitude locations experiencing greater variability in temperature and ocean chemistry (Rohling *et al.,* 2012). The fact that this relationship is not recorded in our planktonic stable isotope records suggest that even high-magnitude environmental signals may be obscured by biological and ecological effects.

The unexpected nature of our results highlights the need for further investigation into the millennial-scale ecology and stable isotope test geochemistry of planktonic foraminifera. The addition of benthic and planktonic Mg/Ca data for our study interval will strengthen our

understanding of the $\delta^{18}O$ records and our interpretations of the unexpected discrepancies found in this study. Work is currently being conducted to model surface ocean temperature and chemistry dynamics across the study interval, and these efforts will help determine the extent to which planktonic foraminiferal stable isotopes can record orbital-scale environmental change during the greenhouse climate of the Middle Eocene.

Acknowledgments

First and foremost, this project was made possible by the guidance and support of Drs. Pincelli Hull and Simon D'haenens. I would also like to thank Drs. Donald Penman and Michael Henehan for their assistance with trace metal analysis and results interpretation. Brad Erkkila of the Yale Analytical and Stable Isotope Center (YASIC) was also instrumental in the collection of stable isotope data, the funding for which was provided by the Yale Institute for Biospheric Studies (YIBS). I would also like to thank Dr. Leanne Elder and her team of lab workers for their help with sample preparation. The SEM images presented here were produced by Paige Breen and Simon D'haenens. Samples were provided by the International Ocean Discovery Program (IODP) Expedition 342, and I would like to thank everyone involved with the sample collection and preparation efforts. Finally, I am extremely grateful for the assistance of the U.C. Santa Cruz Stable Isotope Laboratory for their significant contribution to the stable isotope measurements presented in this study.

References

Birch, H. S., Coxall, H. K., & Pearson, P. N. Evolutionary ecology of Early Paleocene planktonic foraminifera: size, depth habitat and symbiosis. *Paleobiology* 38, 374–390 (2012).

Birch, H. S., Coxall, H. K., Pearson, P. N., Kroon, D. & O'Regan, M. Planktonic foraminifera stable isotopes and water column structure: Disentangling ecological signals. *Marine Micropaleontology* 101, 127–145 (2013).

Bornemann, A., Norris, R. D. Size-related stable isotope changes in Late Cretaceous planktic foraminifera: Implications for paleoecology and photosymbiosis. *Marine Micropaleontology* 65, 32-42 (2007).

Breen, P. M. Creating an extensive, multi-species planktonic isotope record at an Eocene-Oligocene high latitude site. *Undergraduate Senior Thesis*, Department of Geology & Geophysics, Yale University, New Haven, CT (2016).

Broecker, W. S. The Great Ocean Conveyor. *Oceanography* 4, 79-89 (1991).

Burgess, C. E. *et al.* Middle Eocene climate cyclicity in the southern Pacific: Implications for global ice volume. *Geology* 36, 651–4 (2008).

D'haenens, S., Bornemann, A., Roose, K., Claeys, P. & Speijer, R. Stable isotope paleoecology (δ13C and δ18O) of early Eocene Zeauvigerina aegyptiaca from the North Atlantic (DSDP Site 401). *Austrian Journal of Earth Science* 105, 179-188 (2012).

D'Hondt, S., Zachos, J. C. & Schultz, G. Stable isotopic signals and photosymbiosis in late Paleocene planktic foraminifera. *Paleobiology* 20, 391-406 (1994).

Edgar, K. M., Wilson, P. A., Sexton, P. F. & Suganuma, Y. No extreme bipolar glaciation during the main Eocene calcite compensation shift. *Nature* 448, 908–911 (2007).

Elderfield, H., Vautravers, M. & Cooper, M. The relationship between shell size and Mg/Ca, Sr/Ca, δ18O, and δ13C of species of planktonic foraminifera. *Geochemistry, Geophysics, Geosystems* 3, 1–13 (2002).

Emiliani, C. Depth habitats of some species of pelagic Foraminifera as indicated by oxygen isotope ratios. *American Journal of Science* 252, 149–158 (1954).

Erez, J. & Honjo, S. Comparison of isotopic composition of planktonic foraminifera in plankton tows, sediment traps and sediments. *Palaeogeography, Palaeoclimatology, Palaeoecology* 33, 129–156 (1981).

Ezard, T. H. G., Edgar, K. M. & Hull, P. M. Environmental and biological controls on size specific δ13C and δ18O in recent planktonic foraminifera. *Paleoceanography* 30 (2015).

Fallet, U., Brummer, G.J., Zinke, J., Vogels, S. & Ridderinkhof, H. Contrasting seasonal fluxes of planktonic foraminifera and impacts on paleothermometry in the Mozambique Channel upstream of the Agulhas Current. *Paleoceanography* 25, PA4223 (2010).

Friedrich, O. *et al.* Influence of test size, water depth, and ecology on Mg/Ca, Sr/Ca, δ18O and δ13C in nine modern species of planktic foraminifers. *Earth and Planetary Science Letters* 319-320, 133–145 (2012).

Ganssen, G. M. *et al.* Quantifying sea surface temperature ranges of the Arabian Sea for the past 20,000 years. *Clim. Past* 7, 1337–1349 (2011).

Hilting, A. K., Kump, L. R., Bralower, T. J. Variations in the oceanic vertical carbon isotope gradient and their implications for the Paleocene-Eocene biological pump. *Paleoceanography* 23 (2008).

Hull, P. M., Osborn, K. J., Norris, R. D., Robison, B. H. Seasonality and depth distribution of a mesopelagic foraminifer, *Hastigerinella digitata*, in Monterey Bay, California. *Limnol. Oceanogr.* 56, 562–576 (2011).

Hull, P. Collaborative Research: Eocene Orbital-scale Oceanographic Variability in the North Atlantic: Inferences from Expedition 342 Cores. NSF Grant Proposal (2013).

Hull, P. M. *et al.* Data Report: weight percent coarse fraction record for the Eocene megasplice at IODP Sites U1406, U1408, U1409, and U14111. Eocene Stable Isotope Consortium Data Report (2015).

John, E. H. *et al.* Warm ocean processes and carbon cycling in the Eocene. *Philosophical Transactions of the Royal Society of London A* 371, 20130099 (2013).

Killingley, J. S., Johnson, R. F. & Berger, W. H. Oxygen and carbon isotopes of individual shells of planktonic foraminifera from Onton-Java Plateau, equatorial Pacific. *Palaeogeography, Palaeoclimatology, Palaeoecology* 33, 193–204 (1980).

Kump, L. R. Interpreting carbon-isotope excursions: Strangelove oceans. *Geology* 19, 299–302 (1991).

Marsay, C. M. *et al.* Attenuation of sinking particulate organic carbon flux through the mesopelagic ocean. *Proc. Natl. Acad. Sci. U.S.A.* 112, 1089–1094 (2015).

Mohtadi, M. *et al.* Low-latitude control on seasonal and interannual changes in planktonic foraminiferal flux and shell geochemistry off south Java: A sediment trap study. *Paleoceanography* 24 (2009).
Norris, R. D. Symbiosis as an evolutionary innovation in the radiation of Paleocene planktic foraminifera. *Paleobiology* 22, 461-480 (1996).
Norris, R. D. *et al.* Site U1408. *Proceedings of the Integrated Ocean Drilling Program* 342, 1–91 (2014).
Pearson, P. N. Oxygen isotopes in foraminifera: Overview and historical review. *Paleontological Society Papers* 18, 1-38 (2012).
Pearson, P. N. *et al.* Stable warm tropical climate through the Eocene Epoch. *Geology* 35, 211–214 (2007).
Pearson, P. N., Shackleton, N. J. & Hall, M. A. Stable isotope paleoecology of middle Eocene planktonic foraminifera and multi-species isotope stratigraphy, DSDP Site 523, South Atlantic. *Journal of Foraminiferal Research* 23, 123–140 (1993).
Reynolds, L. & Thunell, R. C. Seasonal succession of planktonic foraminifera in the subpolar North Pacific. *Journal of Foraminiferal Research* 15, 282–301 (1985).
Rohling, E. J., Medina-Elizalde, M., Shepherd, J. G., Siddall, M. & Stanford, J. D. Sea Surface and High-Latitude Temperature Sensitivity to Radiative Forcing of Climate over Several Glacial Cycles. *J. Climate* 25, 1635–1656 (2012).
Sautter, L. R. & Thunell, R. C. Seasonal Variability in the δ18O and δ13C of Planktonic Foraminifera from an Upwelling Environment: Sediment Trap Results from the San Pedro Basin, Southern California Bight. *Paleoceanography* 6, 307–334 (1991).
Schiffelbein, P. & Hills, S. Direct assessment of stable isotope variability in planktonic foraminifera populations. *Palaeogeography, Palaeoclimatology, Palaeoecology* 48, 197–213 (1984).
Sexton, P. F., Wilson, P. A. & Pearson, P. N. Microstructural and geochemical perspectives on planktic foraminiferal preservation: "Glassy" versus "Frosty". *Geochemistry, Geophysics, Geosystems* 7, Q12P19 (2006).
Spero, H. J. Do planktic foraminifera accurately record shifts in the carbon isotopic composition of seawater ΣCO2? *Marine Micropaleontology* 19, 275–285 (1992).
Spero, H. J., Bijma, J., Lea, D. W. & Bernis, B. E. Effect of seawater carbonate concentration on foraminiferal carbon and oxygen isotopes. *Oceanographic Literature Review* 6, 951 (1998).
Spero, H. J. & Williams, D. F. Extracting environmental information from planktonic foraminiferal δ 13C data. *Nature*, 717–719 (1988).
Spero, H. J. & Williams, D. F. Opening the carbon isotope 'vital effect' black box 1. Seasonal temperatures in the euphotic zone. *Paleoceanography* 4, 593–601 (1989).
Tedesco, K., Thunell, R., Astor, Y., Muller-Karger, F. The oxygen isotope composition of planktonic foraminifera from the Cariaco Basin, Venezuela: Seasonal and interannual variations. *Marine Micropaleontology* 62, 180-193 (2007).
Via, R. K., Thomas, D. J. Evolution of Atlantic thermohaline circulation: Early Oligocene onset of deep-water production in the North Atlantic. *Geology* 34, 441-444 (2006).
Wade, B. S., Al-Sabouni, N., Hemleben, C. & Kroon, D. Symbiont bleaching in fossil planktonic foraminifera. *Evol. Ecol.* 22, 253–265 (2008).
Williams, D. F., Be, A. W. H, Fairbanks, R. G. Seasonal stable isotopic variations in living planktonic foraminifera from Bermuda plankton tows. *Palaeoceaonography,*

Palaeoclimatology, Palaeoecology 33, 71–102 (1980).
Wit, J. C., Reichart, G. J., A Jung, S. J. & Kroon, D. Approaches to unravel seasonality in sea surface temperatures using paired single-specimen foraminiferal δ18O and Mg/Ca analyses. *Paleoceanography* 25, PA4220 (2010).
Zachos, J., Pagani, M., Sloan, L., Thomas, E. & Billups, K. Trends, rhythms, and aberrations in global climate 65 Ma to present. *Science* 292, 686–693 (2001).

Appendix

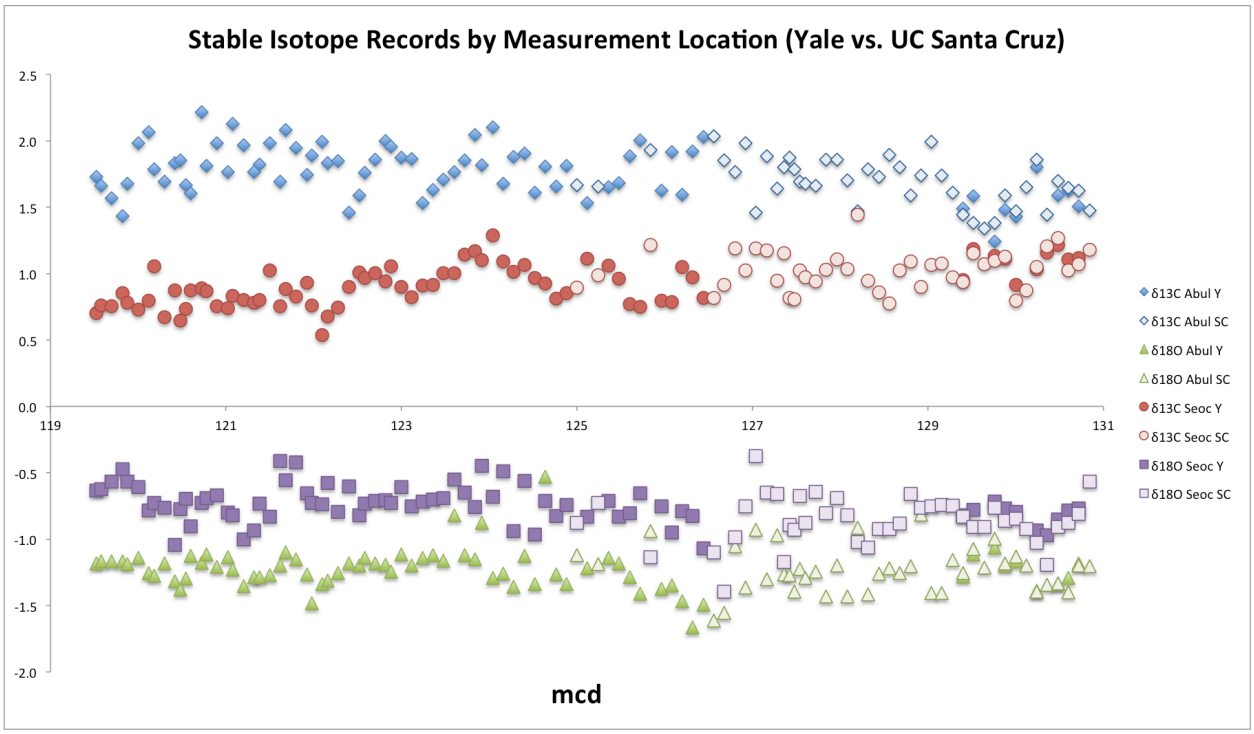

Figure 23. Stable isotope results by measurement location. Dark data points represent measurements made at Yale University. Light data points represent measurements made at the U.C. Santa Cruz Stable Isotope Laboratory.

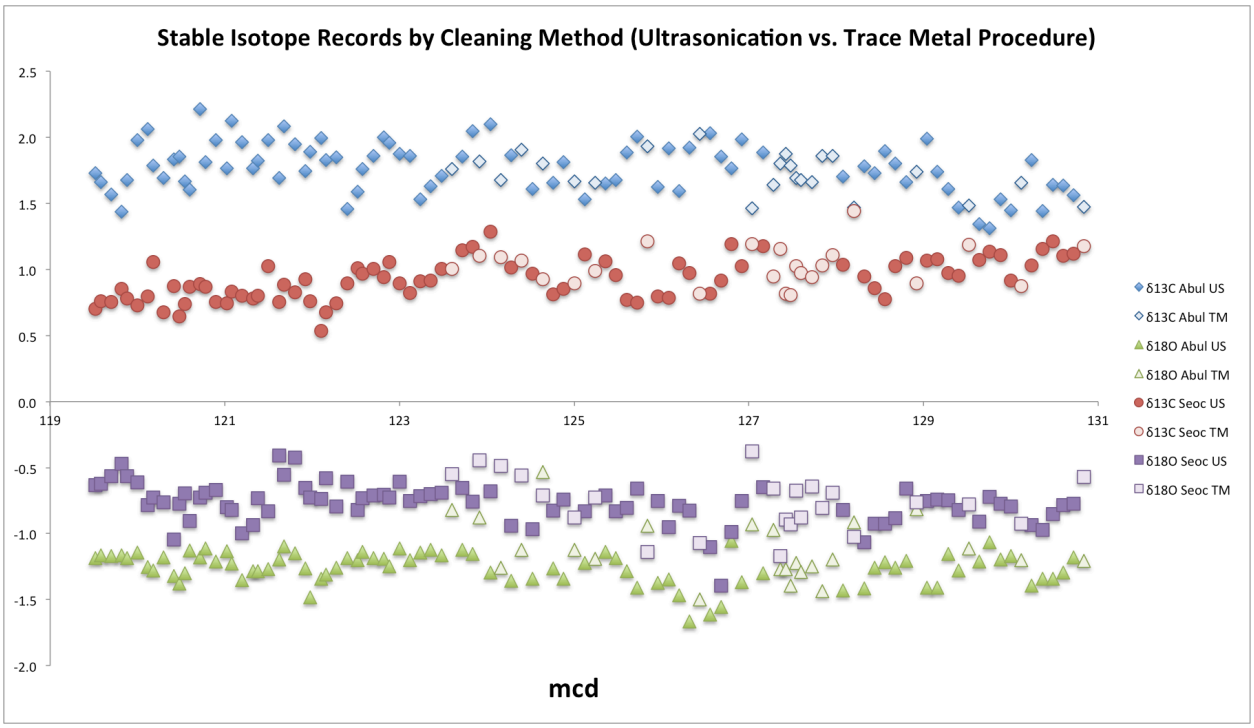

Figure 24. Stable isotope results by sample preparation (cleaning) method. Dark data points represent samples cleaned with ultrasonication. Light data points represent samples cleaned for trace metal analysis.

Table 5. Sample List with Preparation and Measurement Information										
Site	Hole	Core	Section	Half	Top (cm)	Bottom (cm)	mcd	Sampling Method	Cleaning Method	Measurement Location
1408	B	14H	2	W	91	93	119.52	2015	Ultrasonication	Yale
1408	B	14H	2	W	97	99	119.58	2015	Ultrasonication	Yale
1408	B	14H	2	W	109	111	119.7	2015	Ultrasonication	Yale
1408	B	14H	2	W	121	123	119.82	2015	Ultrasonication	Yale
1408	B	14H	2	W	127	129	119.88	2015	Ultrasonication	Yale
1408	B	14H	2	W	139	141	120	2015	Ultrasonication	Yale
1408	B	14H	3	W	1	3	120.12	2015	Ultrasonication	Yale
1408	B	14H	3	W	7	9	120.18	2015	Ultrasonication	Yale
1408	B	14H	3	W	19	21	120.3	2015	Ultrasonication	Yale
1408	B	14H	3	W	31	33	120.42	2015	Ultrasonication	Yale
1408	B	14H	3	W	37	39	120.48	2015	Ultrasonication	Yale
1408	B	14H	3	W	43	45	120.54	2015	Ultrasonication	Yale
1408	B	14H	3	W	49	51	120.6	2015	Ultrasonication	Yale
1408	B	14H	3	W	61	63	120.72	2015	Ultrasonication	Yale
1408	B	14H	3	W	67	69	120.78	2015	Ultrasonication	Yale
1408	B	14H	3	W	79	81	120.9	2015	Ultrasonication	Yale
1408	B	14H	3	W	91	93	121.02	2015	Ultrasonication	Yale
1408	B	14H	3	W	97	99	121.08	2015	Ultrasonication	Yale
1408	B	14H	3	W	109	111	121.2	2015	Ultrasonication	Yale
1408	B	14H	3	W	121	123	121.32	2015	Ultrasonication	Yale
1408	B	14H	3	W	127	129	121.38	2015	Ultrasonication	Yale
1408	B	14H	3	W	139	141	121.5	2015	Ultrasonication	Yale
1408	B	14H	4	W	1	3	121.62	2015	Ultrasonication	Yale
1408	B	14H	4	W	7	9	121.68	2015	Ultrasonication	Yale
1408	B	14H	4	W	19	21	121.8	2015	Ultrasonication	Yale
1408	B	14H	4	W	31	33	121.92	2015	Ultrasonication	Yale
1408	B	14H	4	W	37	39	121.98	2015	Ultrasonication	Yale
1408	B	14H	4	W	49	51	122.1	Both	Ultrasonication	Yale
1408	B	14H	4	W	55	57	122.16	Both	Ultrasonication	Yale
1408	B	14H	4	W	67	69	122.28	Both	Ultrasonication	Yale
1408	B	14H	4	W	79	81	122.4	Both	Ultrasonication	Yale
1408	B	14H	4	W	91	93	122.52	Both	Ultrasonication	Yale
1408	B	14H	4	W	97	99	122.58	2015	Ultrasonication	Yale
1408	B	14H	4	W	109	111	122.7	Both	Ultrasonication	Yale
1408	B	14H	4	W	121	123	122.82	Both	Ultrasonication	Yale
1408	B	14H	4	W	127	129	122.88	Both	Ultrasonication	Yale
1408	B	14H	4	W	139	141	123	Both	Ultrasonication	Yale
1408	B	14H	5	W	1	3	123.12	2016	Ultrasonication	Yale
1408	B	14H	5	W	13	15	123.24	2016	Ultrasonication	Yale
1408	B	14H	5	W	25	27	123.36	2016	Ultrasonication	Yale
1408	B	14H	5	W	37	39	123.48	2016	Ultrasonication	Yale
1408	B	14H	5	W	49	51	123.6	2016	Trace Metal	Yale
1408	B	14H	5	W	61	63	123.72	2016	Ultrasonication	Yale
1408	B	14H	5	W	73	75	123.84	2016	Ultrasonication	Yale
1408	C	14H	2	W	67	69	123.92	2016	Trace Metal	Yale
1408	C	14H	2	W	79	81	124.04	2016	Ultrasonication	Yale
1408	C	14H	2	W	91	93	124.16	2016	Trace Metal	Yale
1408	C	14H	2	W	103	105	124.28	2016	Ultrasonication	Both
1408	C	14H	2	W	115	117	124.4	2016	Trace Metal	Yale
1408	C	14H	2	W	127	129	124.52	2016	Ultrasonication	Yale

1408	C	14H	2	W	139	141	124.64	2016	Trace Metal	Yale
1408	C	14H	3	W	1	3	124.76	2016	Ultrasonication	Yale
1408	C	14H	3	W	13	15	124.88	2016	Ultrasonication	Yale
1408	C	14H	3	W	25	27	125	2016	Ultrasonication	UCSC
1408	C	14H	3	W	37	39	125.12	2016	Ultrasonication	Yale
1408	C	14H	3	W	49	51	125.24	2016	Trace Metal	UCSC
1408	C	14H	3	W	61	63	125.36	2016	Ultrasonication	Yale
1408	C	14H	3	W	73	75	125.48	2016	Ultrasonication	Yale
1408	C	14H	3	W	85	87	125.6	2016	Ultrasonication	Yale
1408	C	14H	3	W	97	99	125.72	2016	Ultrasonication	Yale
1408	C	14H	3	W	109	111	125.84	2016	Trace Metal	UCSC
1408	C	14H	3	W	121	123	125.96	2016	Ultrasonication	Yale
1408	C	14H	3	W	133	135	126.08	2016	Ultrasonication	Yale
1408	C	14H	3	W	145	147	126.2	2016	Ultrasonication	Yale
1408	C	14H	4	W	7	9	126.32	2016	Ultrasonication	Yale
1408	C	14H	4	W	19	21	126.44	2016	Trace Metal	Yale
1408	C	14H	4	W	31	33	126.56	2016	Ultrasonication	UCSC
1408	C	14H	4	W	43	45	126.68	2016	Ultrasonication	UCSC
1408	C	14H	4	W	55	57	126.8	2016	Ultrasonication	UCSC
1408	C	14H	4	W	67	69	126.92	2016	Ultrasonication	UCSC
1408	C	14H	4	W	79	81	127.04	2016	Trace Metal	UCSC
1408	C	14H	4	W	91	93	127.16	2016	Ultrasonication	UCSC
1408	C	14H	4	W	103	105	127.28	2016	Trace Metal	UCSC
1408	A	13H	1	W	121	123	127.36	2016	Trace Metal	UCSC
1408	A	13H	1	W	127	129	127.42	2016	Trace Metal	UCSC
1408	A	13H	1	W	133	135	127.48	2016	Trace Metal	UCSC
1408	A	13H	1	W	139	141	127.54	2016	Trace Metal	UCSC
1408	A	13H	1	W	145	147	127.6	2016	Trace Metal	UCSC
1408	A	13H	2	W	7	9	127.72	2016	Trace Metal	UCSC
1408	A	13H	2	W	19	21	127.84	2016	Trace Metal	UCSC
1408	A	13H	2	W	31	33	127.96	2016	Trace Metal	UCSC
1408	A	13H	2	W	43	45	128.08	2016	Ultrasonication	UCSC
1408	A	13H	2	W	55	57	128.2	2016	Trace Metal	UCSC
1408	A	13H	2	W	67	69	128.32	2016	Ultrasonication	UCSC
1408	A	13H	2	W	79	81	128.44	2016	Ultrasonication	UCSC
1408	A	13H	2	W	91	93	128.56	2016	Ultrasonication	UCSC
1408	A	13H	2	W	103	105	128.68	2016	Ultrasonication	UCSC
1408	A	13H	2	W	115	117	128.8	2016	Ultrasonication	UCSC
1408	A	13H	2	W	127	129	128.92	2016	Trace Metal	UCSC
1408	A	13H	2	W	139	141	129.04	2016	Ultrasonication	UCSC
1408	A	13H	3	W	1	3	129.16	2016	Ultrasonication	UCSC
1408	A	13H	3	W	13	15	129.28	2016	Ultrasonication	UCSC
1408	A	13H	3	W	25	27	129.4	2016	Ultrasonication	Both
1408	A	13H	3	W	37	39	129.52	2016	Trace Metal	Both
1408	A	13H	3	W	49	51	129.64	2016	Ultrasonication	UCSC
1408	A	13H	3	W	61	63	129.76	2016	Ultrasonication	Both
1408	A	13H	3	W	73	75	129.88	2016	Ultrasonication	Both
1408	A	13H	3	W	85	87	130	2016	Ultrasonication	Both
1408	A	13H	3	W	97	99	130.12	2016	Trace Metal	UCSC
1408	A	13H	3	W	109	111	130.24	2016	Ultrasonication	Both
1408	A	13H	3	W	121	123	130.36	2016	Ultrasonication	UCSC

1408	A	13H	3	W	133	135	130.48	2016	Ultrasonication	Both
1408	A	13H	3	W	145	147	130.6	2016	Ultrasonication	Both
1408	A	13H	4	W	7	9	130.72	2016	Ultrasonication	Both
1408	A	13H	4	W	19	21	130.84	2016	Trace Metal	UCSC